Supplementary Information (36 pages)

A co-registered molecular keypad lock for the generation of singlet oxygen

Jialei Chen-Wu,[a] José A. González-Delgado,[a] and Uwe Pischel[a]*

[a] CIQSO – Center for Research in Sustainable Chemistry and Department of Chemistry, University of Huelva, Campus de El Carmen s/n, E-21071 Huelva, Spain

* Corresponding author. Email: uwe.pischel@diq.uhu.es

Table of Contents

1. Materials and methods

General methods

All reagents and solvents for the synthesis were commercially available and used as received without further purification. Column chromatography was performed on silica gel Merck-60 (230–400 mesh, 60 Å) or C18-reversed phase silica gel (550–950 mesh, 100 Å). The ^{1}H, ^{13}C, and ^{19}F NMR measurements as well as 2D NMR were done either on a Bruker Advanced 400 MHz HPPR2 or a Bruker Advanced 500 MHz HPPR2 instrument. High-resolution mass spectra were obtained on a Bruker Compact Elite QTOF with an electrospray ionization source (ESI) by positive mode.

Photochemical and photophysical methods

All measurements were done at room temperature (25 ºC) with air-equilibrated solutions contained in quartz cuvettes with 1 cm optical pathlength. Acetone, the solvent used for these measurements, was purchased in the highest-purity spectroscopic grade. For the photoswitching experiments a TLC lamp (Vilber Lourmat-6.LC, 365 nm) or a 150 W xenon lamp (Oriel GmbH & Co. KG) either with a 550-nm optical long-pass filter or a 580-nm bandpass filter were employed. UV/vis absorption measurements were done with an Agilent Cary 5000 spectrophotometer. Fluorescence spectra and time-correlated single-photon-counting (TCSPC) measurements were performed with an Edinburgh Instruments FLS 920 fluorimeter. As excitation source a picosecond pulsed diode laser EPLED-330 (output 334.6 nm, pulse width at FWHM: 200 ns) was employed. Fluorescence lifetimes were obtained by deconvolution analysis of the decay curves, taking into account the instrument response function. The latter was determined with a light-scattering Ludox solution. Fluorescence quantum yields were determined with an integrating sphere in a FluoTime 300 spectrometer (PicoQuant). Singlet oxygen

phosphorescence measurements were done with a FluoTime 300 spectrometer equipped with a CW Xenon lamp as excitation source and a NIR-PMTs detector.

Rose Bengal (Φ_Δ = 0.70 in acetone)[1] was used as reference to determine the efficiency of singlet-oxygen formation. The quantum yields of the DTE ring closing and ring opening were determined by employing appropriate actinometers and using the method of the initial rate. For this, the open forms were irradiated at 365 nm and potassium tri-oxalatoferrate(III)trihydrate was used (Φ_r = 1.21 in a buffer solution of 0.23 M CH_3COONa / 0.05 M H_2SO_4),[2, 3] while the closed forms were irradiated at 580 nm and 1,2-bis(2,4-dimethyl-5-phenyl-3-thienyl)-3,3,4,4,5,5-hexafluoro-1-cyclopentene was employed as actinometer (Φ_r = 0.0173 in *n*-hexane).[4, 5]

The occurrence of FRET in **1c** was substantiated by applying the Förster theory.[6] The spectral overlap integral was determined with the "pure" DTE-related absorption spectrum of **1c**, obtained by subtracting the contribution of the anthracene chromophore, represented by the spectrum of the model compound **3**. The fluorescence spectrum of **1o** was used in the calculation of the spectral overlap integral $J_{\text{dipole – dipole.}}$ The critical FRET radius R_0 was then determined according to equation 1. The fluorescence quantum yield of the anthracene, not quenched by FRET, was approximated using the value obtained for **3**. Finally, the theoretically expected Φ_{FRET} was calculated with equation 2.

$$R_0{}^6 = \frac{9 \ln 10 \kappa^2 \Phi_{\text{donor}}}{128 \pi^5 n^4 N_A} J_{\text{dipole – dipole}} \quad (1)$$

$$\Phi_{\text{FRET}} = \frac{1}{1 + \left(\frac{R}{R_0}\right)^6} \quad (2)$$

2. Synthesis and characterization

Compound **DTE-I_2** was prepared following a reported procedure.[7]

Note: All DTE-containing compounds were obtained as ring-open isomers.

Synthesis of 4-(4-(3,3,4,4,5,5-hexafluoro-2-(5-iodo-2-methylthiophen-3-yl)cyclopent-1-en-1-yl)-5-methylthiophen-2-yl)pyridine (A1)

An oven-dried 100 mL Schlenk tube was charged with **DTE-I_2** (500.0 mg, 0.80 mmol), 4-pyridinylboronic acid (123.0 mg, 1.00 mmol), Na_2CO_3 (340.0 mg, 3.20 mmol), and $Pd(PPh_3)_4$ (100.0 mg, 0.09 mmol) under nitrogen atmosphere. Both deoxygenated 1,2-dimethoxyethane (20.0 mL) and water (7.0 mL) were added to the solid mixture *via* a cannula and the reaction mixture was heated at 90 ºC for 24 h. After cooling to room temperature, the reaction was quenched by addition of water (115 mL) and diethylether (30 mL). The aqueous layer was further extracted with diethylether (3 × 25 mL) and the combined organic phase was dried over anhydrous Na_2SO_4. After filtration the solvent was evaporated under reduced pressure and the crude product was purified by column chromatography on silica gel (*n*-hexane/ethyl acetate 4:1, v/v), affording **A1** (120.0 mg, 30% yield) as an amorphous colorless solid. ^{1}H NMR (400 MHz, CD_2Cl_2) δ 8.61–8.53 (m, 2H), 7.46 (s, 1H), 7.43–7.39 (m, 2H), 7.25 (s, 1H), 1.98 (s, 3H), 1.93 (s, 3H) ppm. ^{13}C{^{1}H} NMR (101 MHz, CD_2Cl_2) δ 150.5 (2C), 148.1, 143.9, 140.0, 139.3, 136.1, 126.5, 125.8, 124.6, 119.4 (2C), 70.8, 14.5, 14.1 ppm (the signals corresponding to the perfluorinated cyclopentene are not visible). ^{19}F NMR (376 MHz, CD_2Cl_2) δ –110.4, –110.6, –132.2 (p, J = 5.5 Hz) ppm. HRMS (ESI, QTOF) *m/z* calcd for $C_{20}H_{13}F_6INS_2$ $[M+H]^+$ 571.9433; found $[M+H]^+$ 571.9431.

Synthesis of (4-(4-(3,3,4,4,5,5-hexafluoro-2-(2-methyl-5-(pyridin-4-yl)thiophen-3-yl)cyclopent-1-en-1-yl)-5-methylthiophen-2-yl)phenyl)methanamine (A2)

An oven-dried 100 mL Schlenk tube was charged with **A1** (120.0 mg, 0.21 mmol), 4-(aminomethyl)phenylboronic acid pinacol ester hydrochloride (113.2 mg, 0.42 mmol), Na_2CO_3 (90.0 mg,0.84 mmol), $Pd(PPh_3)_4$ (25.0 mg, 0.02 mmol), and XPhos (19.0 mg, 0.04 mmol) under nitrogen atmosphere. Both deoxygenated 1,2-dimethoxyethane (10.0 mL) and water (3.0 mL) were added to the solid mixture *via* a cannula and the reaction mixture was heated at 90 ºC for 24 h. After cooling to room temperature, the reaction was quenched by addition of water (50 mL) and diethylether (20 mL). The aqueous layer was further extracted with diethylether (3 × 20 mL) and the combined organic phase was dried over anhydrous Na_2SO_4. After filtration the organic solvent was evaporated under reduced pressure and the crude product was purified by column chromatography on C18-reversed phase silica gel (100% acetonitrile to 100% methanol gradient) affording **A2** (52.0 mg, 45% yield) as an amorphous colorless solid. ^{1}H NMR (500 MHz, $CDCl_3$) δ 8.62–8.58 (m, 2H), 7.51 (d, J = 8.4 Hz, 2H), 7.48 (s, 1H), 7.43–7.38 (m, 2H), 7.34 (d, J = 8.4 Hz, 2H), 7.25 (s, 1H), 3.90 (s, 2H), 2.01 (s, 3H), 1.96 (s, 3H) ppm. ^{13}C{^{1}H} NMR (126 MHz, $CDCl_3$) δ 150.7 (2C), 143.4, 142.5, 140.4, 132.0, 127.9 (2C), 126.6, 125.9 (2C), 125.0, 122.2, 119.7 (2C), 46.3, 14.9, 14.7 ppm (the signals corresponding to the perfluorinated cyclopentene are not visible). ^{19}F NMR (470 MHz, $CDCl_3$) δ –110.0, –110.1, –131.8 (p, J = 5.2 Hz) ppm. HRMS (ESI, QTOF) *m/z* calcd for $[M+H]^+$ 551.1045. $C_{27}H_{21}F_6N_2S_2$; found $[M+H]^+$ 551.1041.

Synthesis of 2-(4-(4-(3,3,4,4,5,5-hexafluoro-2-(2-methyl-5-(pyridin-4-yl)thiophen-3-yl)cyclopent-1-en-1-yl)-5-methylthiophen-2-yl)benzyl)-1*H*-naphtho[2,3-*f*]isoindole-1,3(2H)-dione (A3)

An oven-dried 100 mL Schlenk tube was charged with **A2** (50.0 mg, 0.09 mmol) and 2,3-anthracenedicarboxylic anhydride (45.0 mg, 0.18 mmol) under nitrogen atmosphere. Deoxygenated ethanol (5.0 mL) was added to the solid mixture *via* a cannula and the reaction mixture was heated at 85 ºC for 24 h. After cooling to room temperature the solvent was evaporated, the solid residue was dissolved in dichloromethane, and the organic phase was washed several times with water. The organic phase was dried over anhydrous Na_2SO_4. After filtration the solvent was evaporated under reduced pressure and the crude product was purified by column chromatography on silica gel (*n*-hexane/ethyl acetate 1:1, v/v), affording **A3** (25.0 mg, 36%) as an amorphous blue solid. The blue color is due to the presence of a very minor amount of the ring-closed form. ^{1}H NMR (500 MHz, $CDCl_3$) δ 8.64 (s, 2H), 8.59 (m, 2H), 8.52 (s, 2H), 8.11–8.06 (m, 2H), 7.65–7.61 (m, 2H), 7.54–7.47 (m, 4H), 7.46 (s, 1H), 7.39 (m, 2H), 7.22 (s, 1H), 4.95 (s, 2H), 1.97 (s, 3H), 1.95 (s, 3H) ppm. ^{13}C{^{1}H} NMR (126 MHz, $CDCl_3$) δ 167.6 (2C), 150.7 (2C), 143.8, 142.2, 141.5, 140.4, 139.2, 136.4, 133.5 (2C), 133.0, 132.1 (2C), 130.3 (2C), 129.7 (2C), 128.6 (2C), 127.8 (2C), 126.7 (2C), 126.5, 126.3 (2C), 126.1 (2C), 125.8, 125.0, 122.6, 119.7 (2C), 41.7, 14.9, 14.7 ppm (the signals corresponding to the perfluorinated cyclopentene are not visible). ^{19}F NMR (470 MHz, $CDCl_3$) δ –110.0, –110.1, –131.9 (p, J = 5.2 Hz) ppm. HRMS (ESI, QTOF) *m/z* calcd for $C_{43}H_{27}F_6N_2O_2S_2$ $[M+H]^+$ 781.1413; found $[M+H]^+$ 781.1425.

Synthesis of 4-(4-(2-(5-(4-((1,3-dioxo-1,3-dihydro-2H-naphtho[2,3-f]isoindol-2-yl)methyl)phenyl)-2-methylthiophen-3-yl)-3,3,4,4,5,5-hexafluorocyclopent-1-en-1-yl)-5-methylthiophen-2-yl)-1-methylpyridin-1-ium iodide (1)

An oven-dried 10 mL Schlenk tube was charged with **A3** (25.0 mg, 0.03 mmol) and dry dichloromethane (1.5 mL) under nitrogen atmosphere. Subsequently, methyl iodide (0.5 mL, 8.0 mmol) was added dropwise into the solution of **A3**, and the reaction mixture was stirred at room temperature for 72 h. The resulting suspension was filtered and the solid was washed several times with dichloromethane and dried *in vacuo* to afford **1** (17.0 mg, 56% yield) as an amorphous green solid. The green color is due to the presence of a very minor amount of the ring-closed form. ^{1}H NMR (500 MHz, CD_3OD) δ 8.81 (s, 2H), 8.73 (d, J = 7.2 Hz, 2H), 8.62 (s, 2H), 8.22 (d, J = 7.2 Hz, 2H), 8.16 (dd, J = 6.6, 3.2 Hz, 2H), 8.12 (s, 1H), 7.66 (dd, J = 6.6, 3.2 Hz, 2H), 7.56 (d, J = 8.4 Hz, 2H), 7.47 (d, J = 8.4 Hz, 2H), 7.33 (s, 1H), 4.94 (s, 2H), 4.30 (s, 3H), 2.15 (s, 3H), 2.04 (s, 3H) ppm. ^{13}C{^{1}H} NMR (126 MHz, CD_3OD) δ 169.0 (2C), 151.4, 149.4, 146.7 (2C), 143.9, 143.0, 138.2, 136.6, 134.9 (2C), 133.8, 133.4 (2C), 132.6, 131.4 (2C), 130.1 (2C), 129.6 (2C), 129.0, 128.8 (2C), 127.8 (2C), 127.2 (2C), 126.8 (2C), 126.5, 123.6, 123.4 (2C), 47.8, 42.3, 15.1, 14.6 ppm (the signals corresponding to the perfluorinated cyclopentene are not visible). ^{19}F NMR (470 MHz, CD_3OD) δ –111.6, –111.9, –133.5 (p, J = 5.2, 4.8 Hz) ppm. HRMS (ESI, QTOF) *m/z* calcd for $C_{44}H_{29}F_6N_2O_2S_2$ requires $[M–I]^+$ 795.1569; found $[M–I]^+$ 795.1566.

Synthesis of 4-(4-(3,3,4,4,5,5-hexafluoro-2-(5-iodo-2-methylthiophen-3-yl)cyclopent-1-en-1-yl)-5-methylthiophen-2-yl)-1-methylpyridin-1-ium iodide (2)

An oven-dried 10 mL Schlenk tube was charged with **A1** (30.0 mg, 0.05 mmol) and dry dichloromethane (1.5 mL) under a nitrogen atmosphere. Subsequently, methyl iodide (0.5 mL, 8.0 mmol) was added dropwise into the solution of **A1**, and the reaction mixture was stirred at room temperature for 72 h. The resulting mixture was precipitated with diethylether, the suspension was filtered, and the solid was washed several times with diethylether and vacuum-dried to afford **2** (20.0 mg, 54% yield) as an amorphous green solid. The green color is due to the presence of a very minor amount of the ring-closed form. ^{1}H NMR (400 MHz, CD_2Cl_2) δ 9.01 (d, J = 6.9 Hz, 2H), 8.03 (d, J = 6.9 Hz, 2H), 7.82 (s, 1H), 7.23 (s, 1H), 4.53 (s, 3H), 2.07 (s, 3H), 1.96 (s, 3H). ^{13}C{^{1}H} NMR (101 MHz, CD_2Cl_2) δ 151.2, 148.8, 148.6, 145.7 (2C), 136.3, 135.2, 131.1, 128.2, 126.5, 122.8 (2C), 72.0, 48.8, 15.5, 14.8 (the signals corresponding to the perfluorinated cyclopentene are not visible). ^{19}F NMR (376 MHz, CD_2Cl_2) δ –110.2, –110.7, –132.1 (p, J = 5.2 Hz). HRMS (ESI, QTOF) *m/z* calcd for $C_{21}H_{15}F_6INS$ $[M–I]^+$ 585.9589; found $[M–I]^+$ 585.9563.

Synthesis of 2-benzyl-1*H*-naphtho[2,3-*f*]isoindole-1,3(2*H*)-dione (3)

An oven-dried 100 mL Schlenk tube was charged with benzylamine (55.0 mg, 0.5 mmol) and 2,3-anthracenedicarboxylic anhydride (125.0 mg, 0.5 mmol) under nitrogen atmosphere. Deoxygenated ethanol (5.0 mL) was added to the solid mixture *via* a cannula and the reaction mixture was heated at 85 ºC for 24 h. After cooling to room temperature the solvent was evaporated, the solid residue was dissolved in dichloromethane, and washed several times with water. The organic phase was dried over anhydrous Na_2SO_4. After filtration the solvent was evaporated under reduced

pressure and the crude product was purified by column chromatography on silica gel (*n*-hexane/ethyl acetate 1:1, v/v), affording **3** (100.0 mg, 60% yield) as an amorphous yellow solid. ^{1}H NMR (400 MHz, $CDCl_3$) δ 8.63 (s, 2H), 8.51 (s, 2H), 8.08 (dd, J = 6.5, 3.2 Hz, 2H), 7.62 (dd, J = 6.5, 3.2 Hz, 2H), 7.54–7.48 (m, 2H), 7.35–7.31 (m, 2H), 7.30–7.27 (m, 1H), 4.95 (s, 2H) ppm. ^{13}C{^{1}H} NMR (101 MHz, $CDCl_3$) δ 167.7 (2C), 136.5 (2C), 133.4 (2C), 132.1 (2C), 130.3 (2C), 128.9 (2C), 128.8 (2C), 128.6 (2C), 128.0, 127.7 (2C), 126.8, 126.2 (2C), 42.1 ppm. HRMS (ESI, QTOF) *m/z* calcd for $C_{23}H_{15}NO_2Na$ $[M+Na]^+$ 360.0995; found $[M+Na]^+$ 360.0980.

3. Characterization by NMR spectroscopy

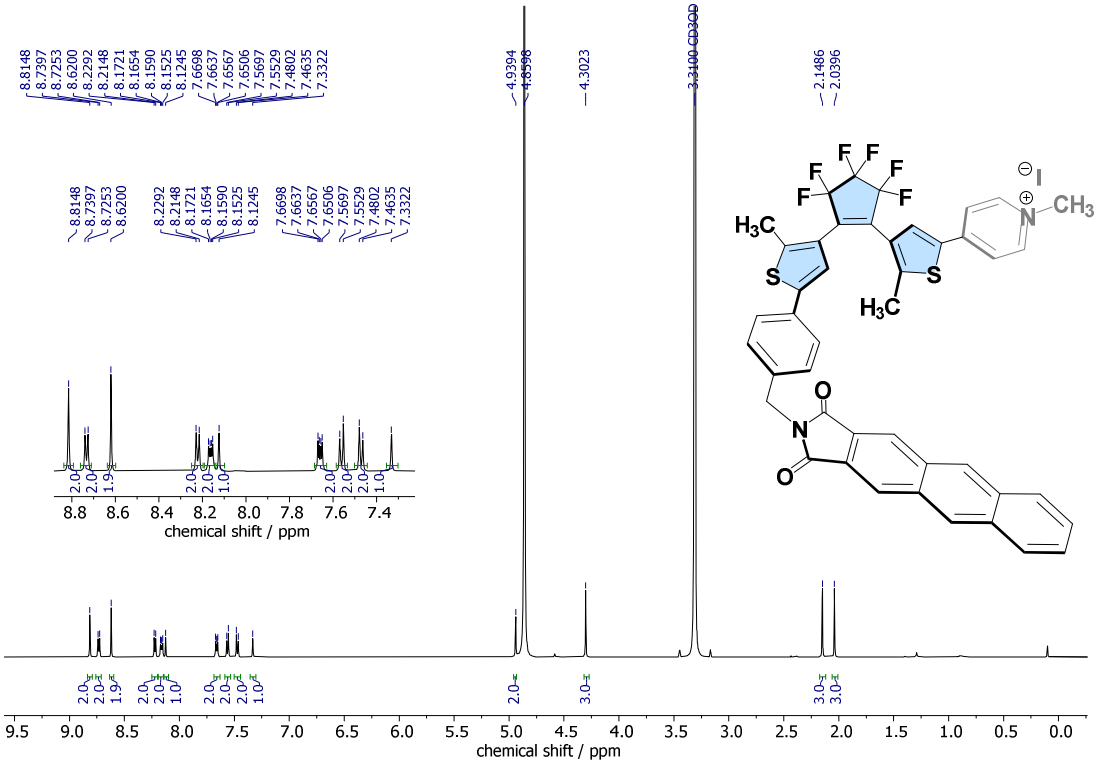

Figure S1. ^{1}H NMR spectrum (500 MHz) of **1** in CD_3OD at 298 K. The inset shows the aromatic signal region between 8.90−7.30 ppm.

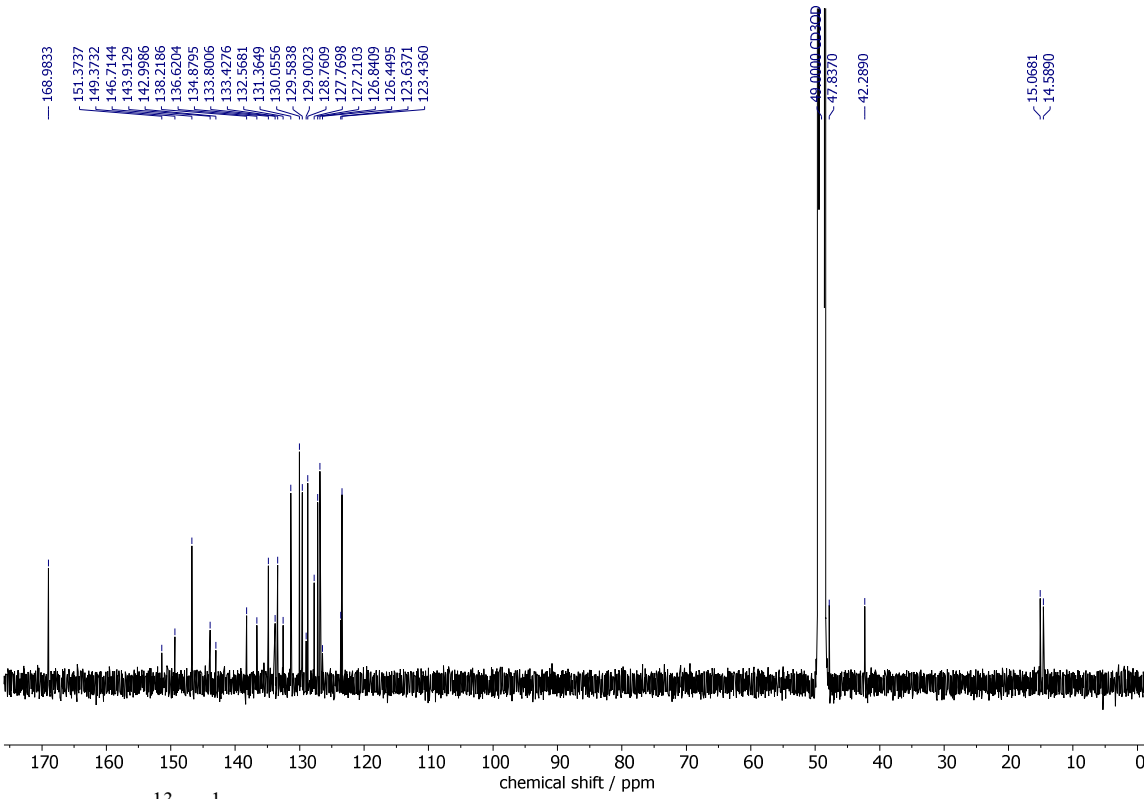

Figure S2. $^{13}C\{^{1}H\}$ NMR spectrum (126 MHz) of **1** in CD_3OD at 298 K.

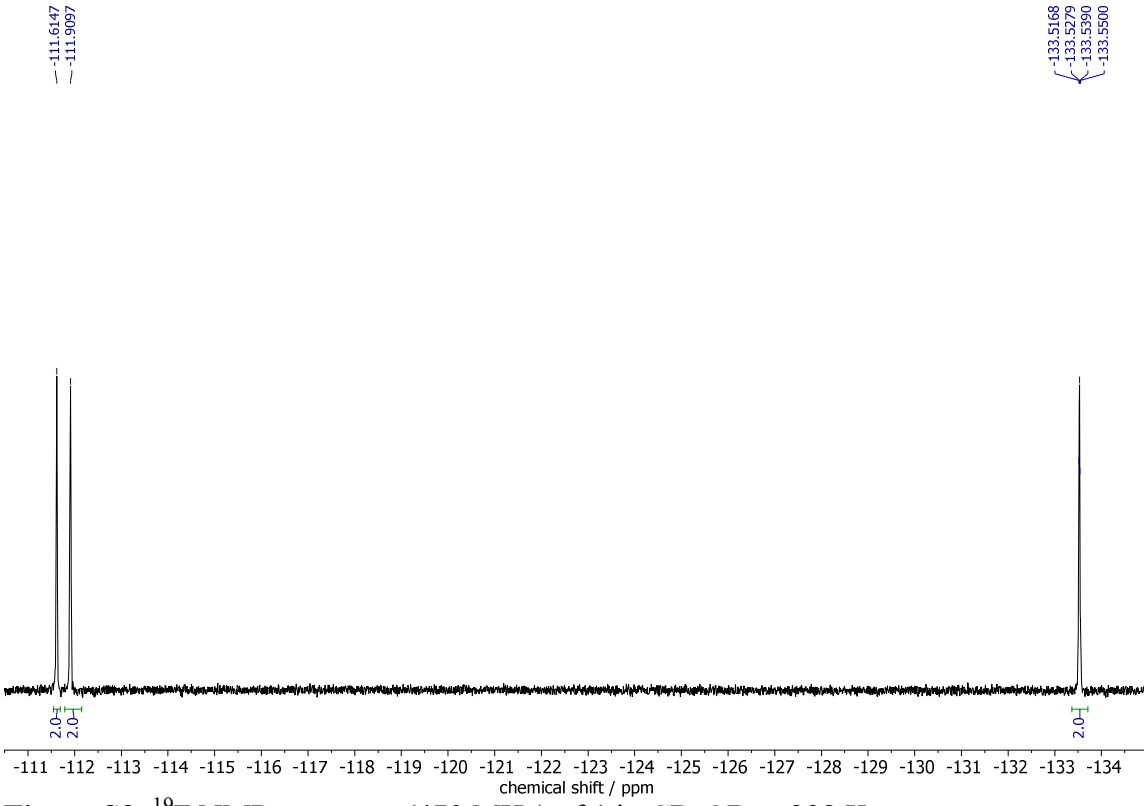

Figure S3. ^{19}F NMR spectrum (470 MHz) of **1** in CD_3OD at 298 K.

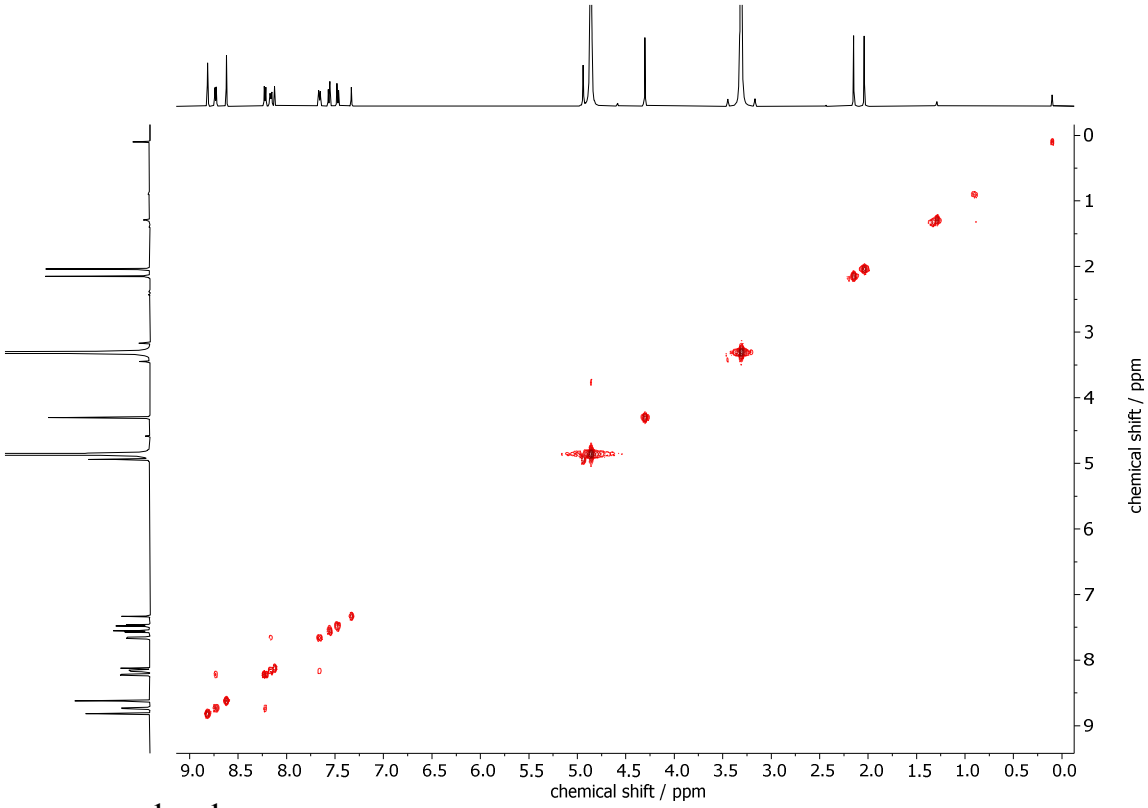

Figure S4. ^{1}H–^{1}H COSY spectrum (500 MHz) of **1** in CD_3OD at 298 K.

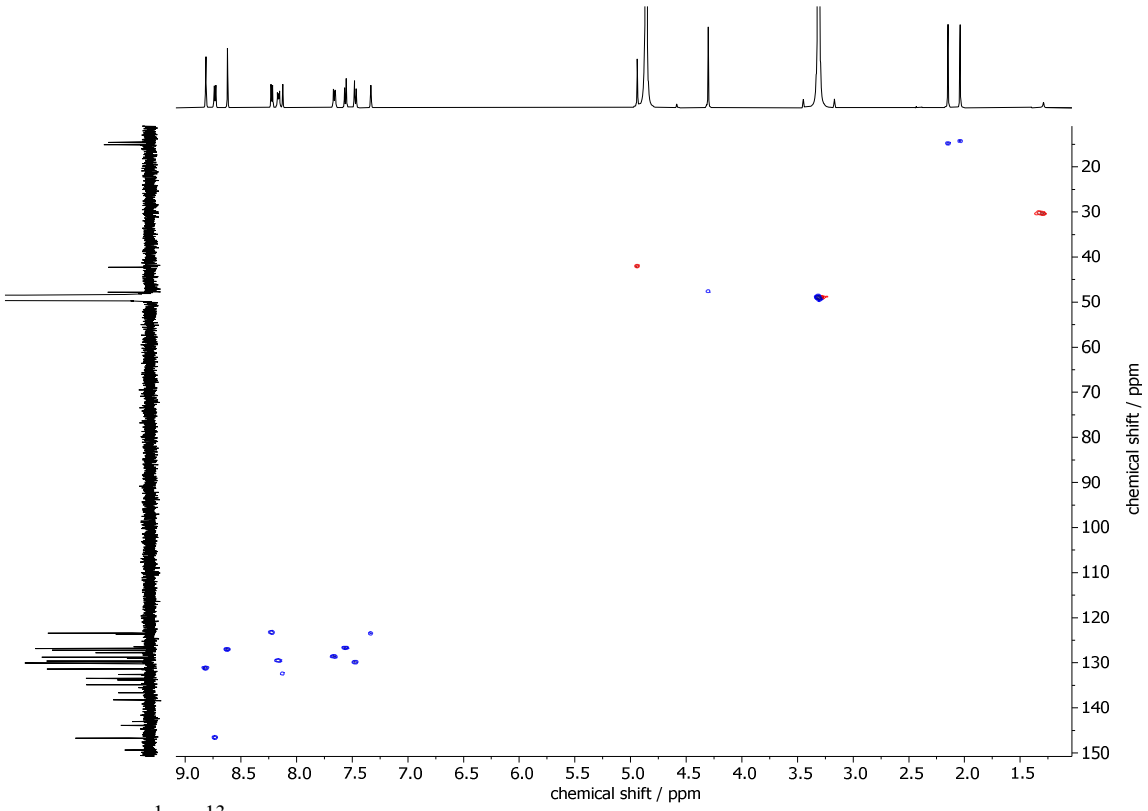

Figure S5. ^{1}H–^{13}C HSQC spectrum (500 MHz) of **1** in CD_3OD at 298 K.

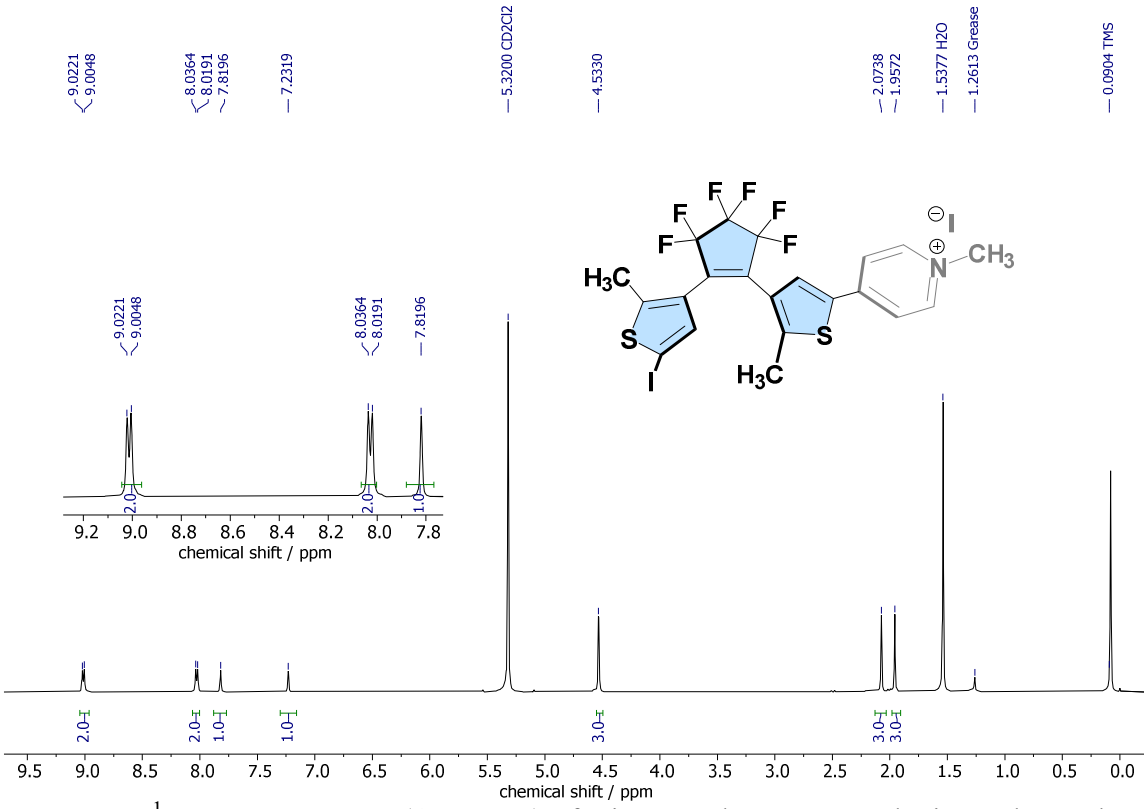

Figure S6. ^{1}H NMR spectrum (400 MHz) of **2** in CD_2Cl_2 at 298 K. The inset shows the aromatic signal region between 9.20−7.80 ppm.

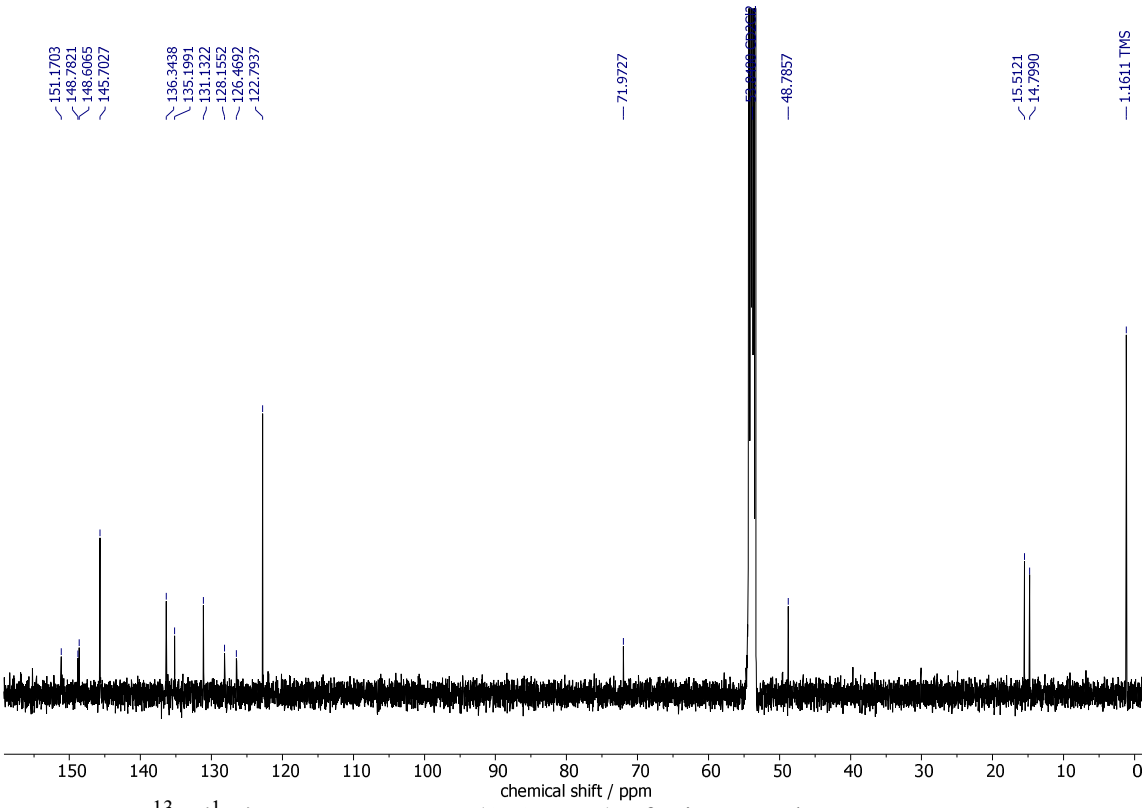

Figure S7. $^{13}C\{^{1}H\}$ NMR spectrum (101 MHz) of **2** in CD_2Cl_2 at 298 K.

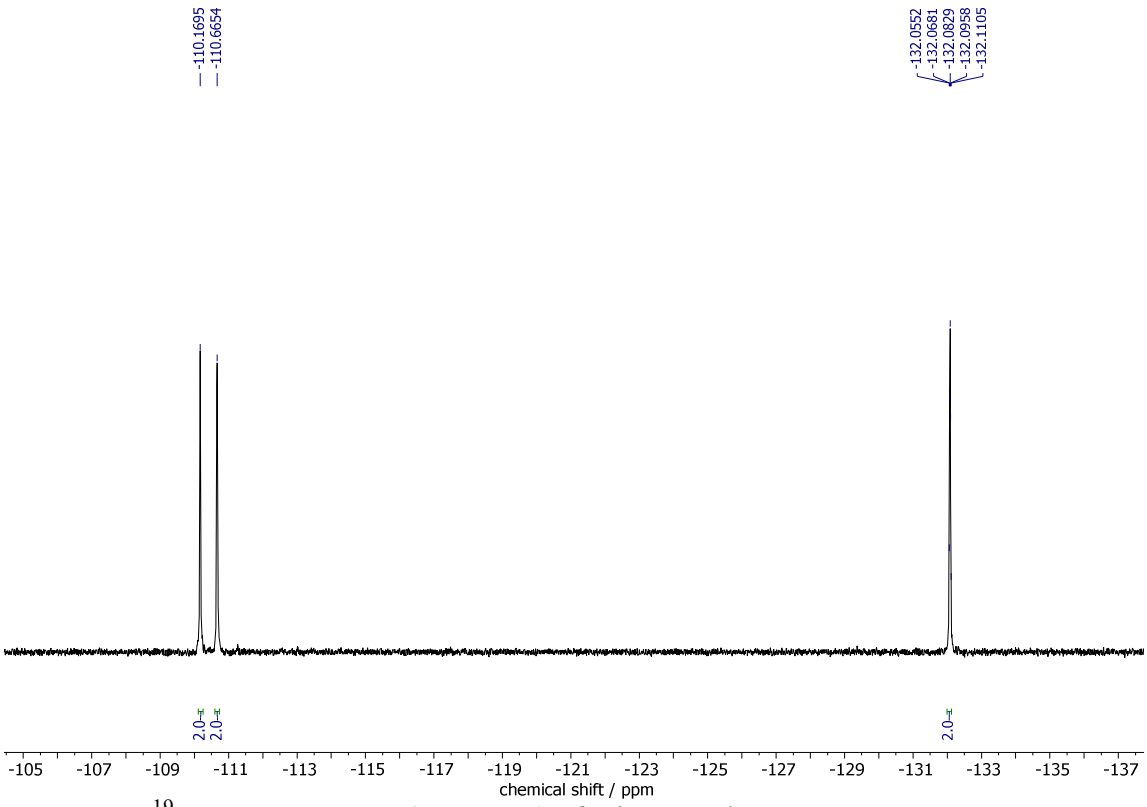

Figure S8. ^{19}F NMR spectrum (376 MHz) of **2** in CD_2Cl_2 at 298 K.

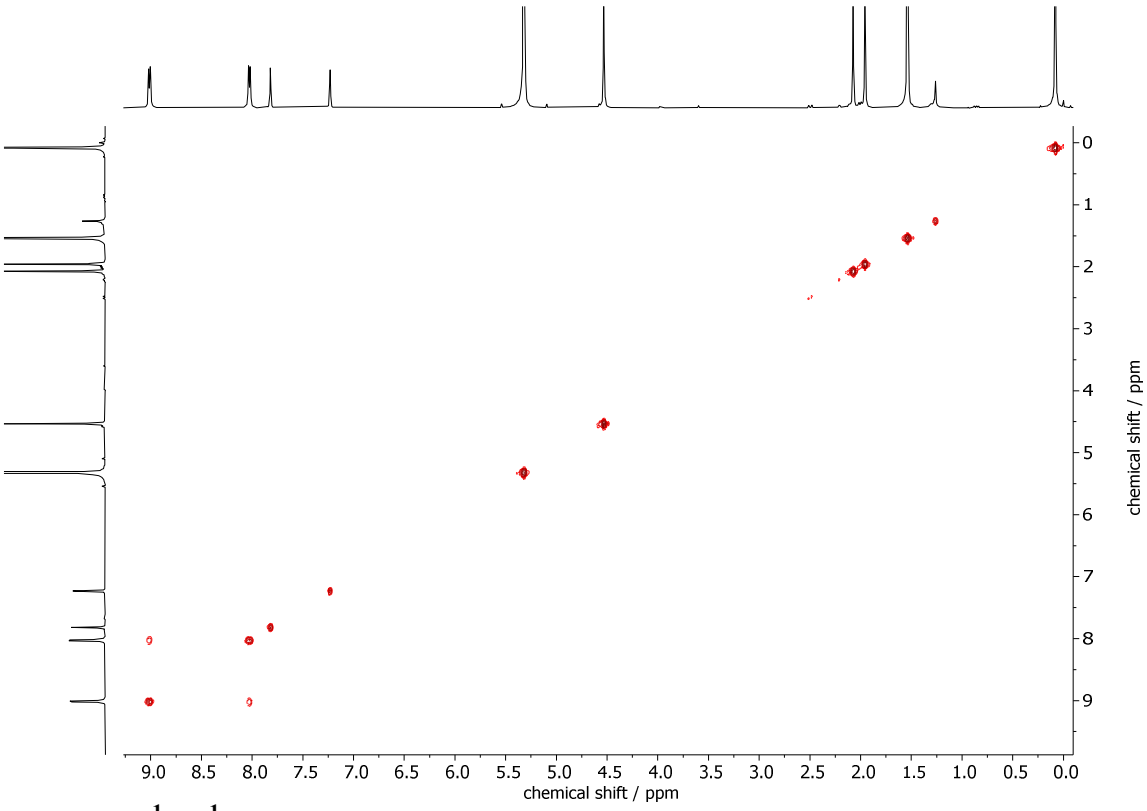

Figure S9. $^{1}H–^{1}H$ COSY spectrum (400 MHz) of **2** in CD_2Cl_2 at 298 K.

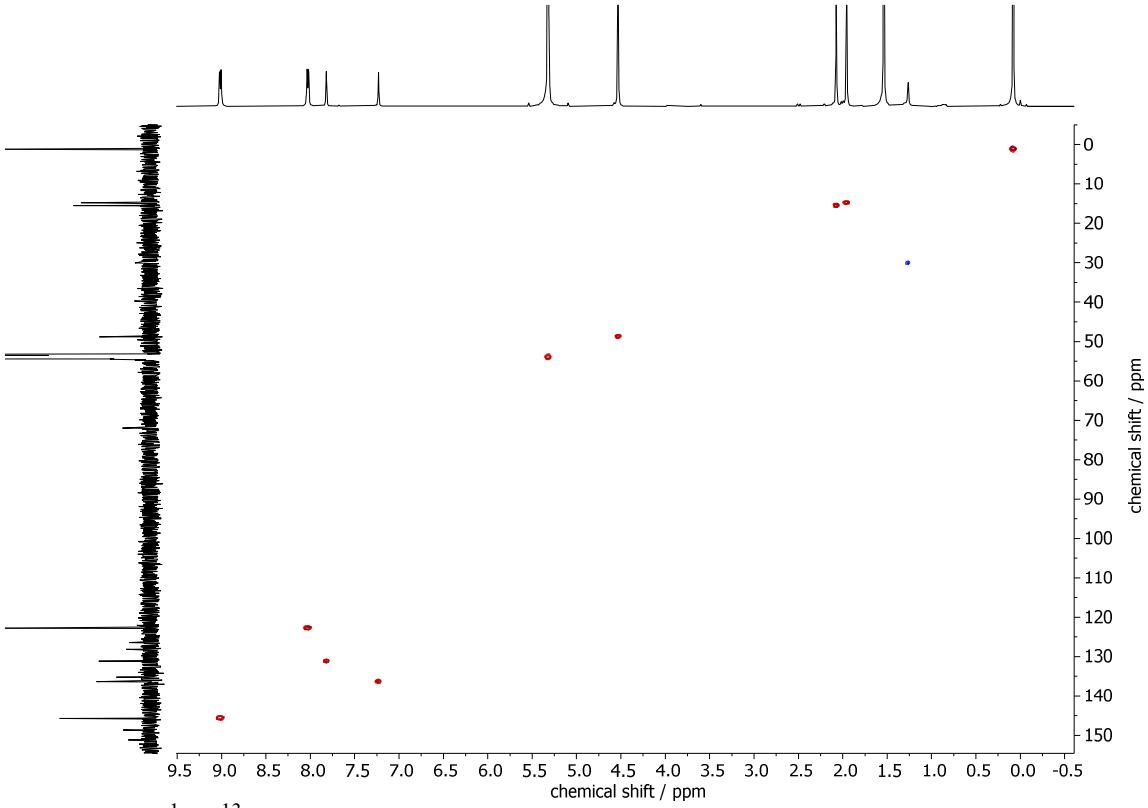

Figure S10. $^{1}H–^{13}C$ HSQC spectrum (400 MHz) of **2** in CD_2Cl_2 at 298 K.

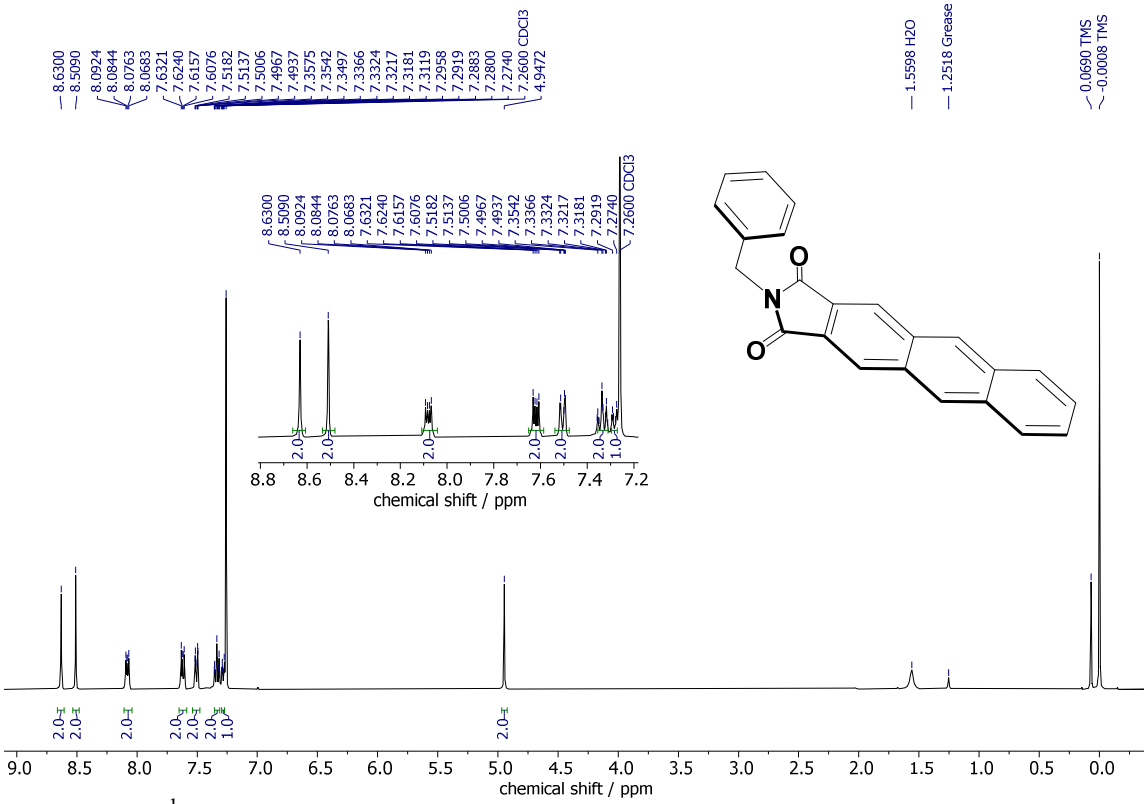

Figure S11. ^{1}H NMR spectrum (400 MHz) of **3** in $CDCl_3$ at 298 K. The inset shows the aromatic signal region between 8.80−7.20ppm.

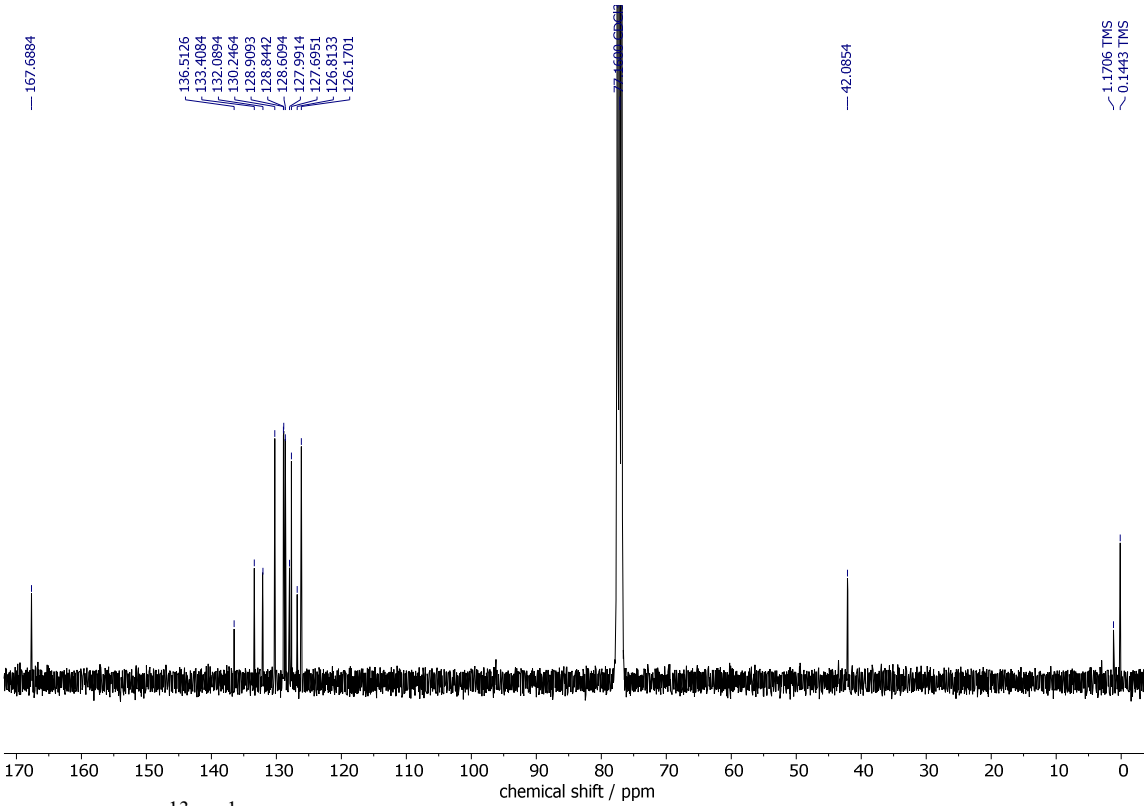

Figure S12. ^{13}C{^{1}H} NMR spectrum (101 MHz) of **3** in $CDCl_3$ at 298 K.

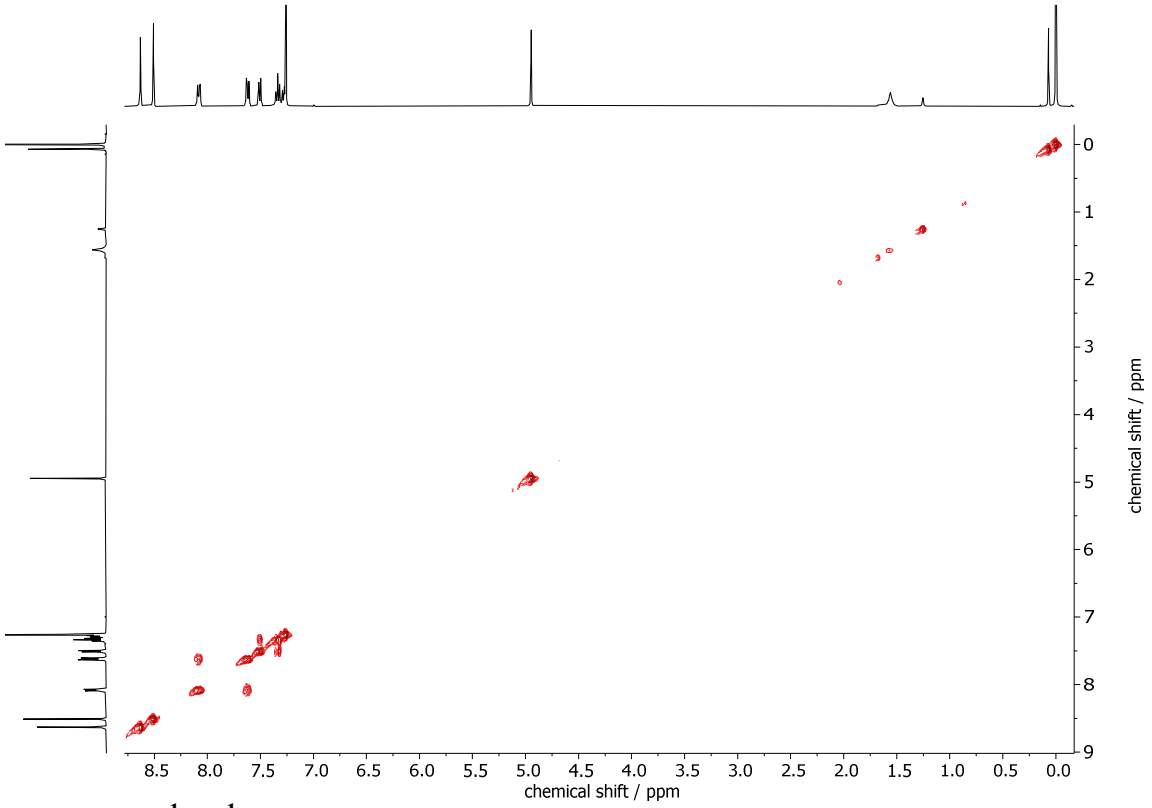

Figure S13. ^{1}H– ^{1}H COSY spectrum (400 MHz) of **3** in $CDCl_3$ at 298 K.

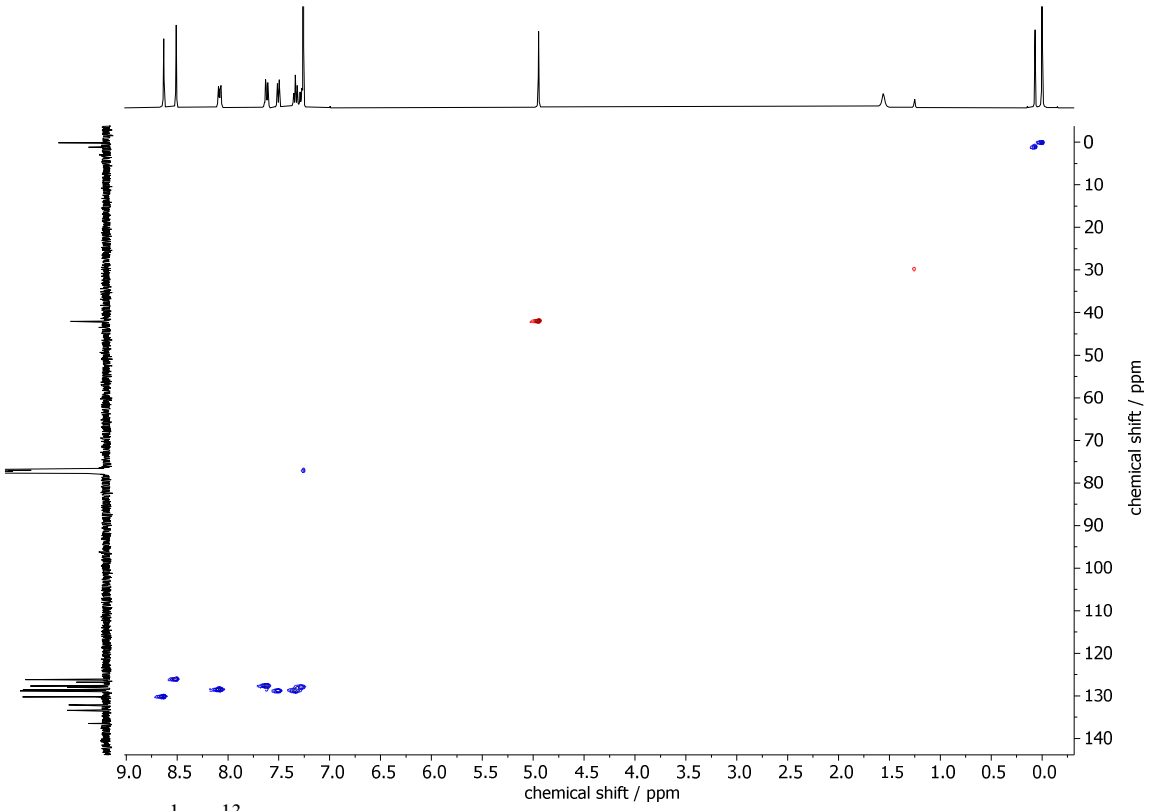

Figure S14. ^{1}H–^{13}C HSQC spectrum (400 MHz) of **3** in $CDCl_3$ at 298 K.

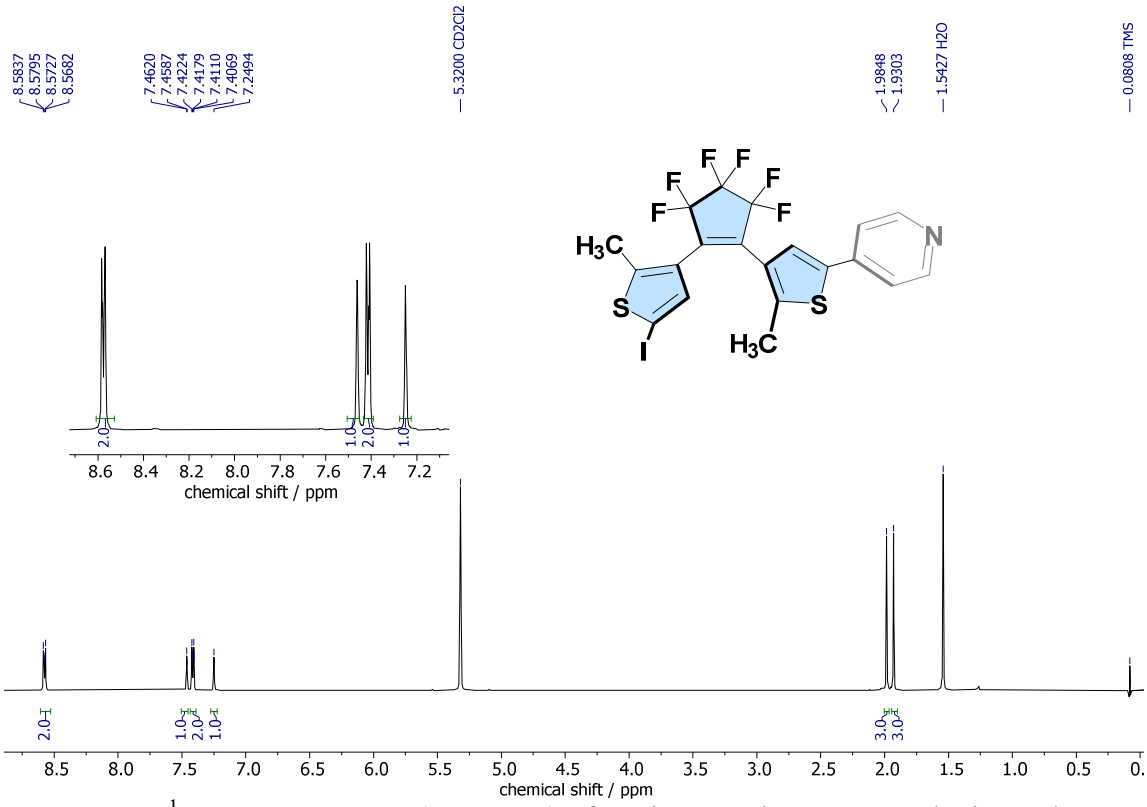

Figure S15. ^{1}H NMR spectrum (400 MHz) of **A1** in CD_2Cl_2 at 298 K. The inset shows the aromatic signal region between 8.70−7.10ppm.

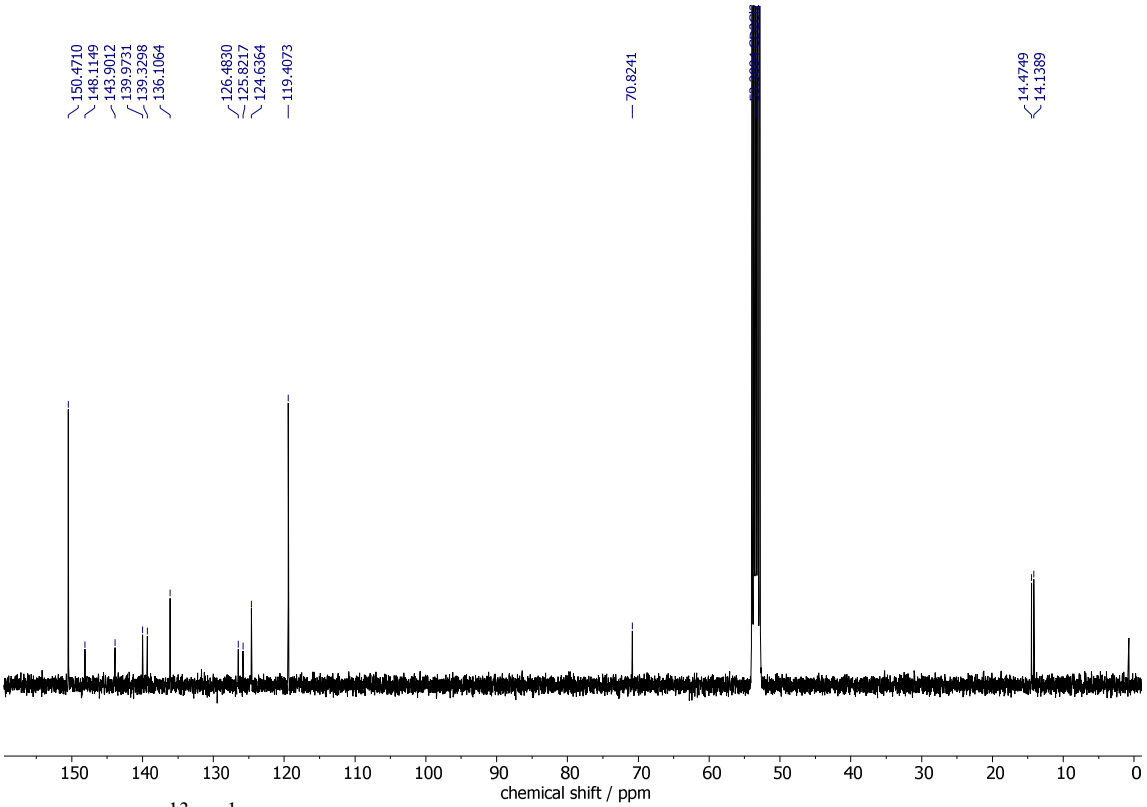

Figure S16. ^{13}C{^{1}H} NMR spectrum (101 MHz) of **A1** in CD_2Cl_2 at 298 K.

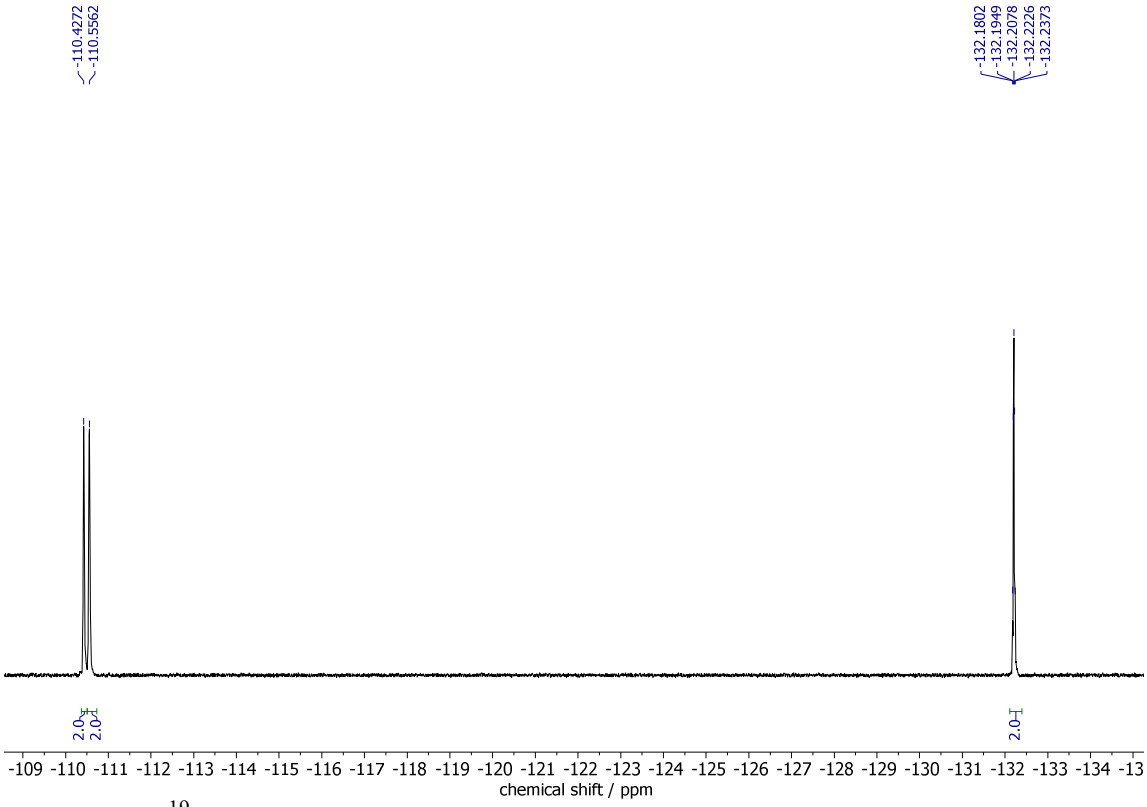

Figure S17. ^{19}F NMR spectrum (376 MHz) of **A1** in CD_2Cl_2 at 298 K.

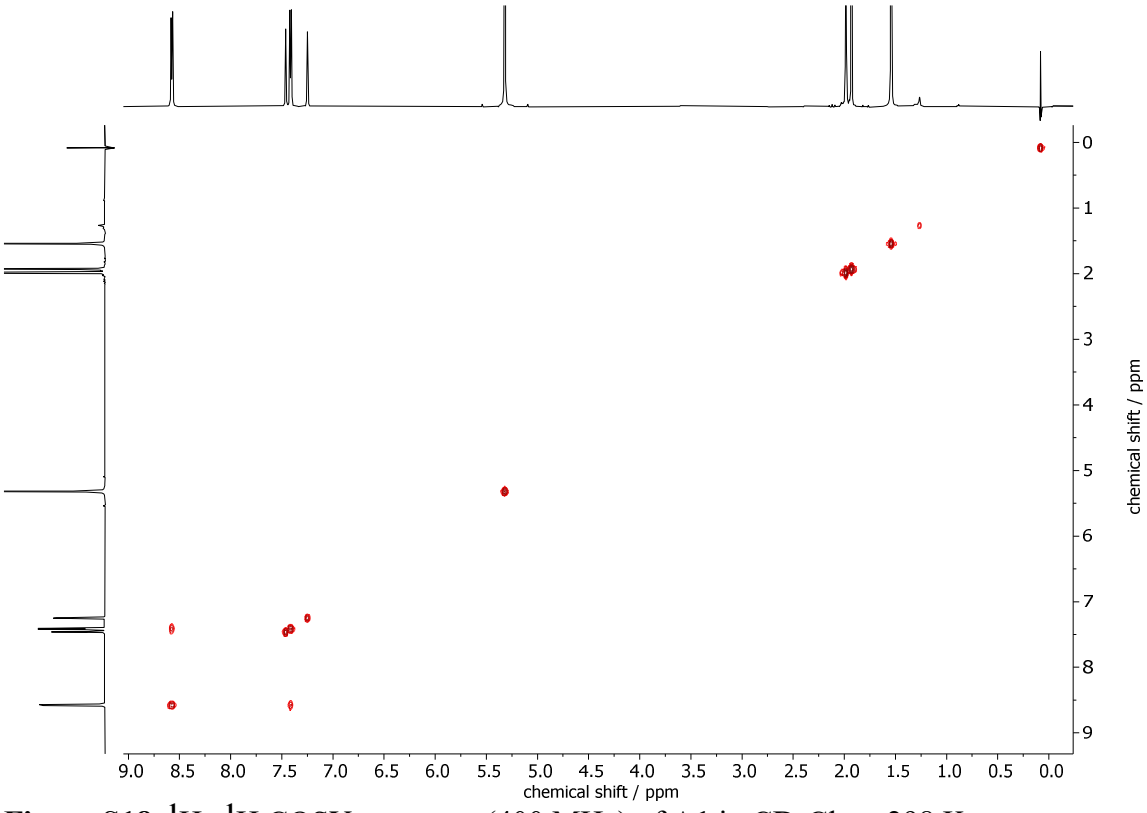

Figure S18. ^{1}H– ^{1}H COSY spectrum (400 MHz) of **A1** in CD_2Cl_2 at 298 K.

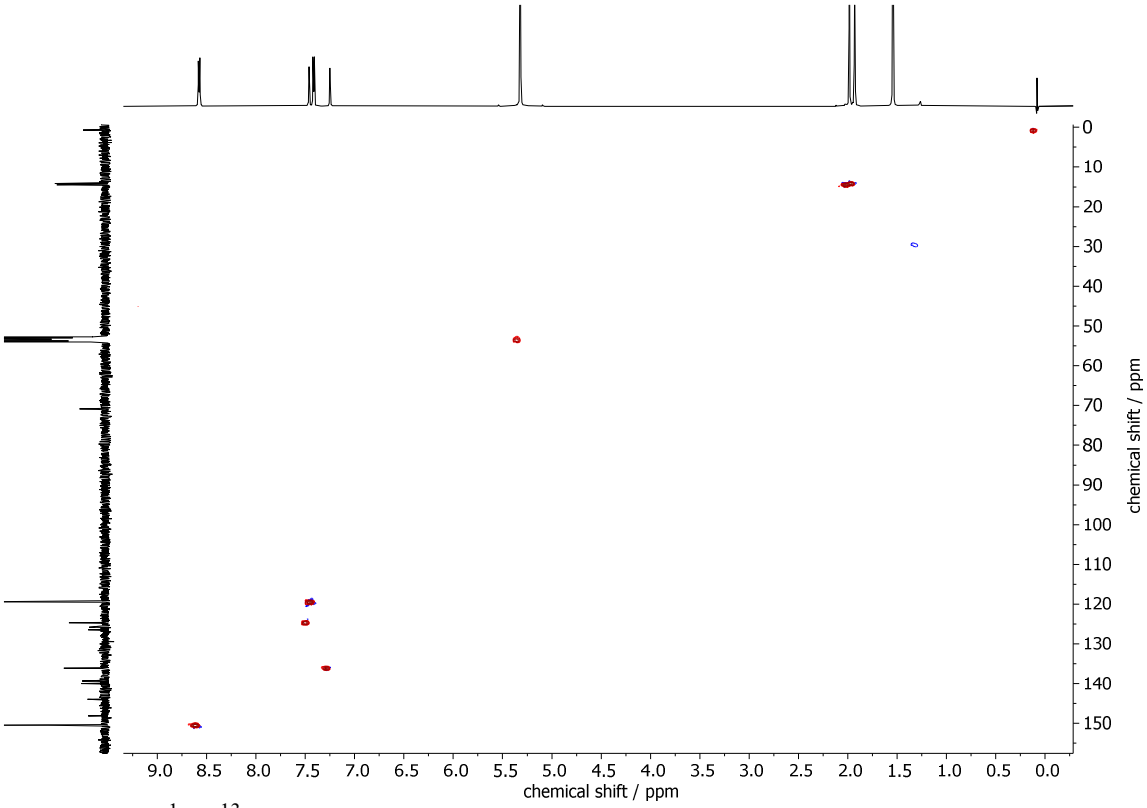

Figure S19. $^{1}H–^{13}C$ HSQC spectrum (400 MHz) of **A1** in CD_2Cl_2 at 298 K.

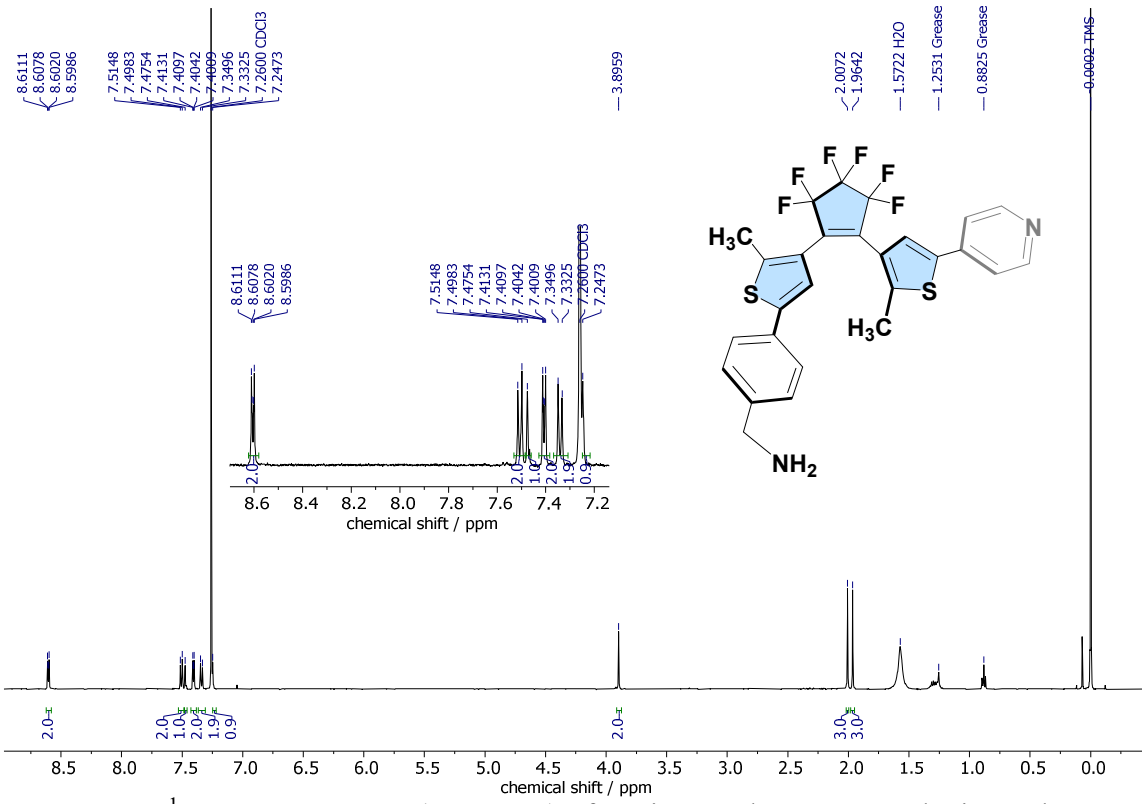

Figure S20. ^{1}H NMR spectrum (500 MHz) of **A2** in $CDCl_3$ at 298 K. The inset shows the aromatic signal region between 8.70−7.20ppm.

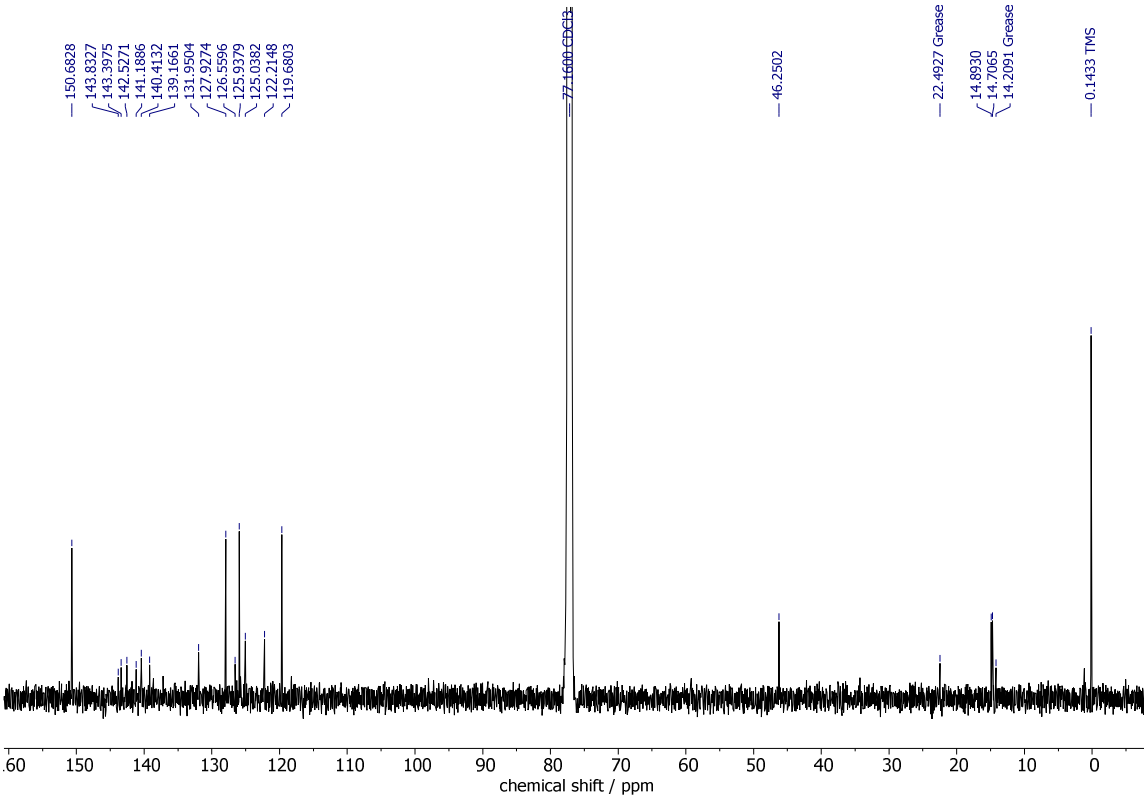

Figure S21. $^{13}C\{^{1}H\}$ NMR spectrum (126 MHz) of **A2** in $CDCl_3$ at 298 K.

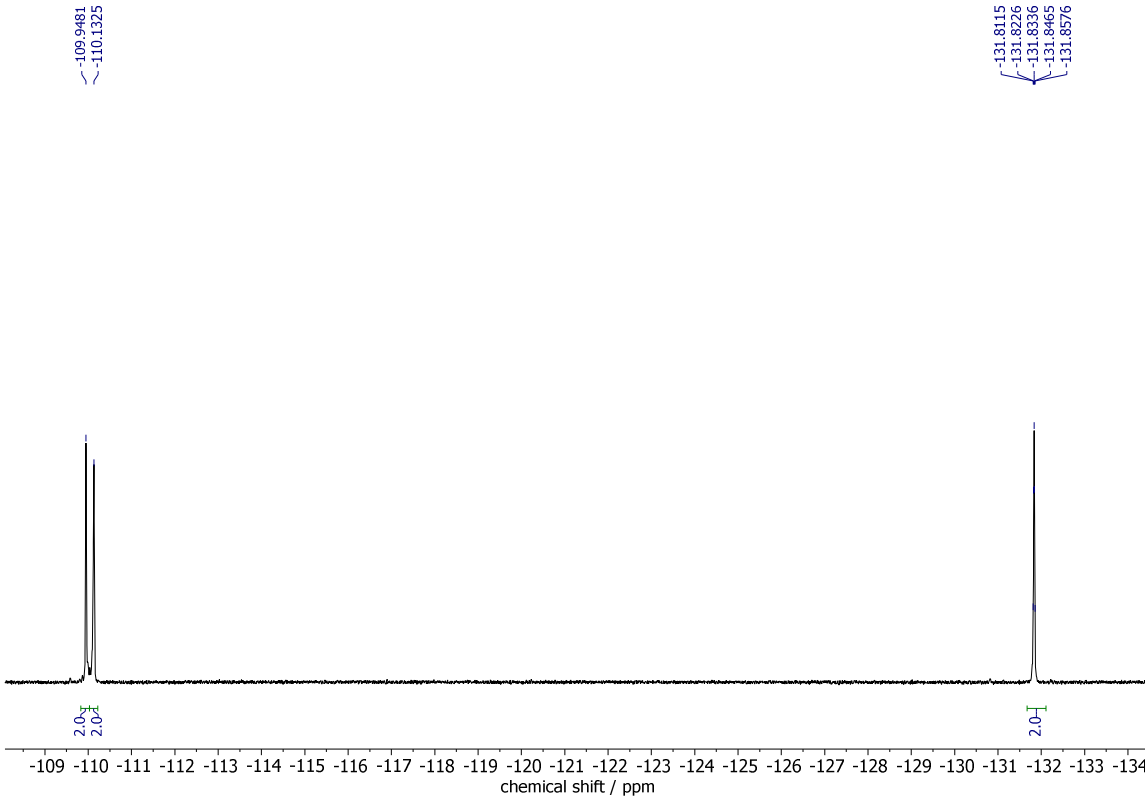

Figure S22. ^{19}F NMR spectrum (470 MHz) of **A2** in $CDCl_3$ at 298 K.

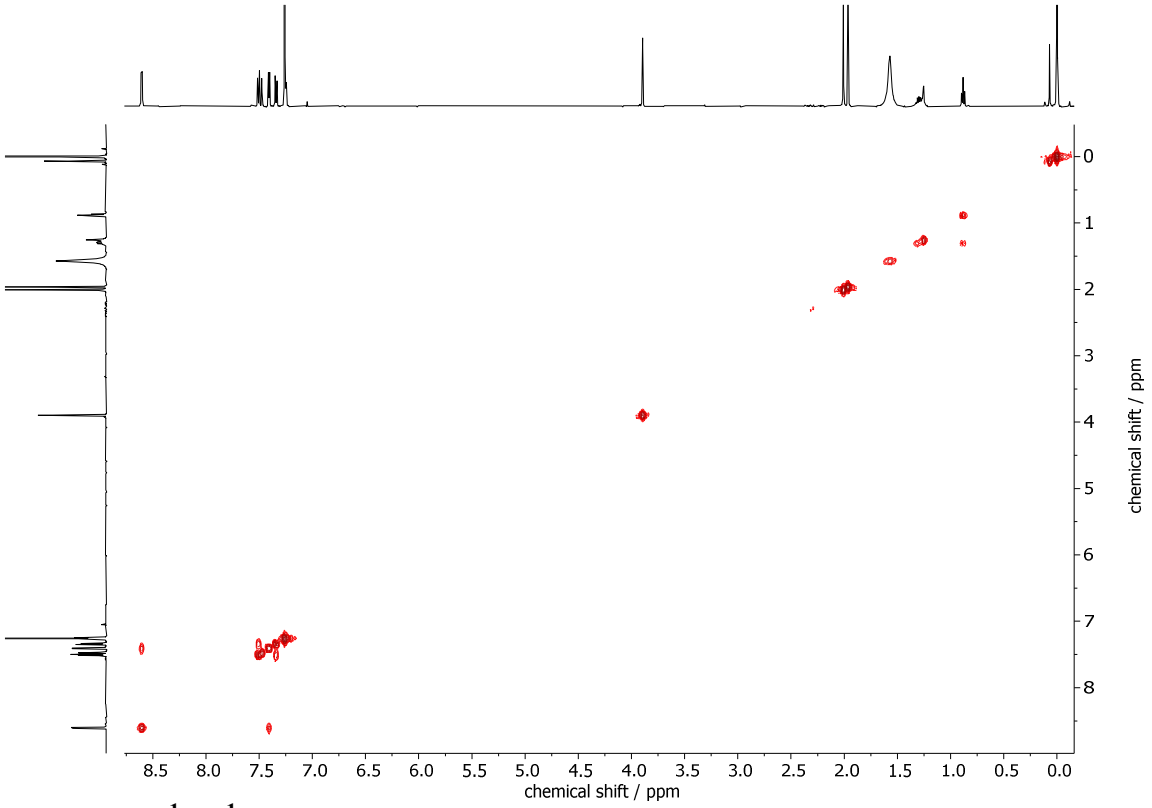

Figure S23. ^{1}H– ^{1}H COSY spectrum (500 MHz) of **A2** in $CDCl_3$ at 298 K.

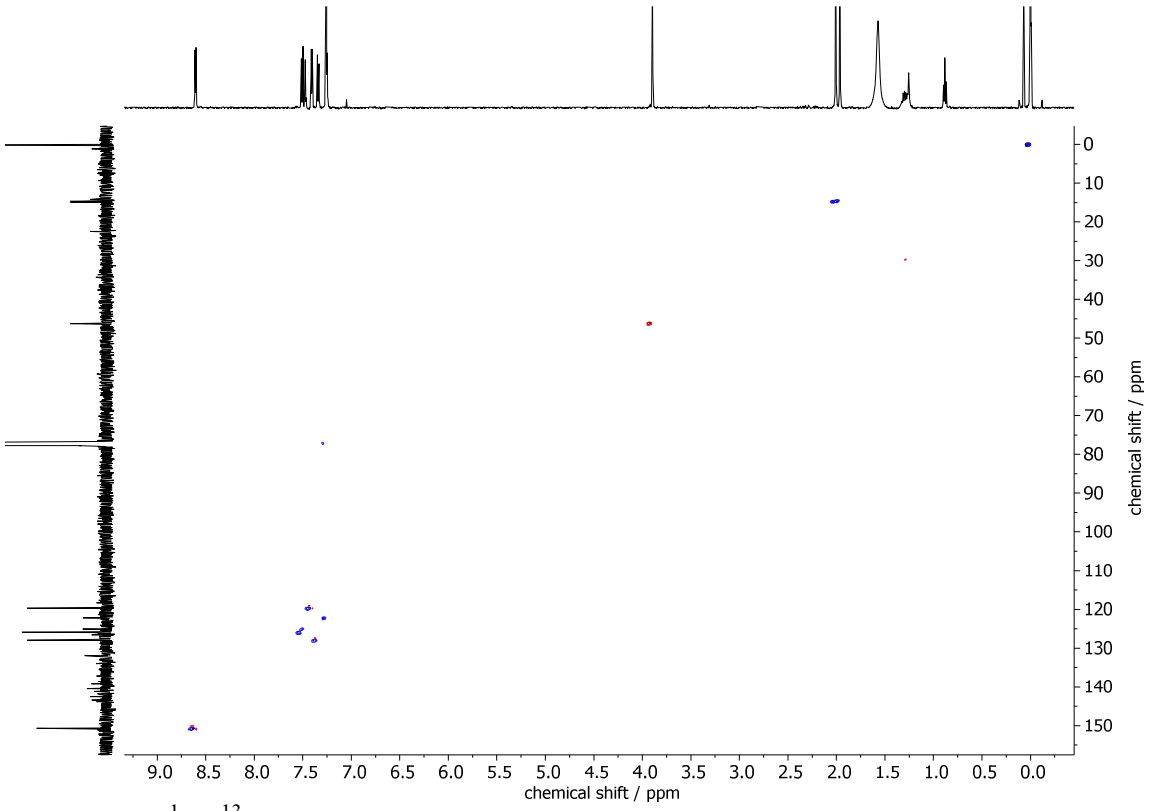

Figure S24. ^{1}H–^{13}C HSQC spectrum (500 MHz) of **A2** in $CDCl_3$ at 298 K.

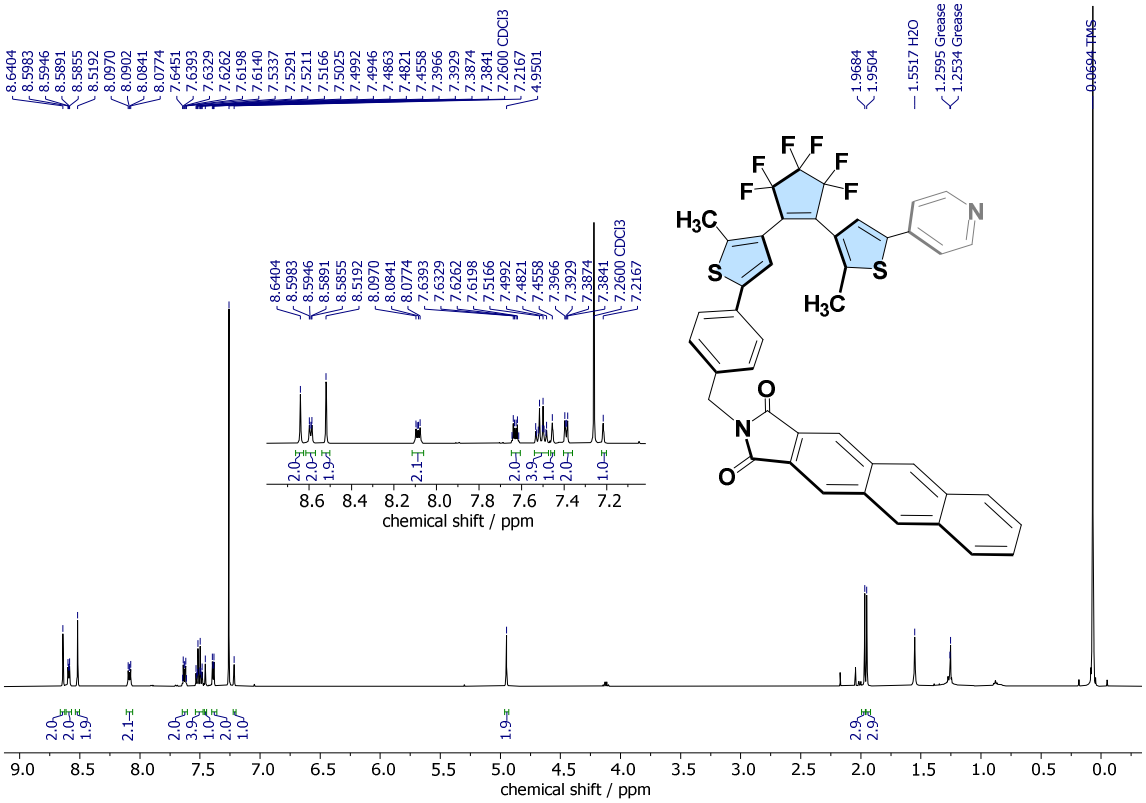

Figure S25. ^{1}H NMR spectrum (500 MHz) of **A3** in $CDCl_3$ at 298 K. The inset shows the aromatic signal region between 8.80−7.10ppm.

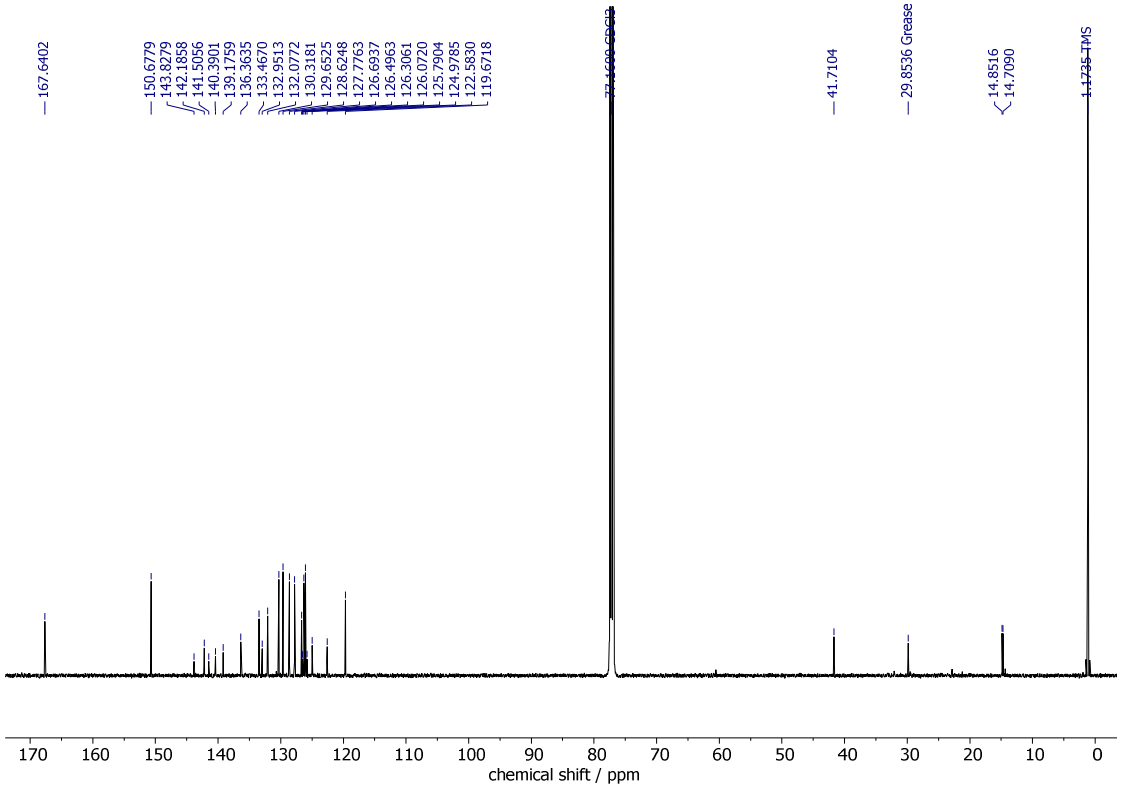

Figure S26. $^{13}C\{^{1}H\}$ NMR spectrum (126 MHz) of **A3** in $CDCl_3$ at 298 K.

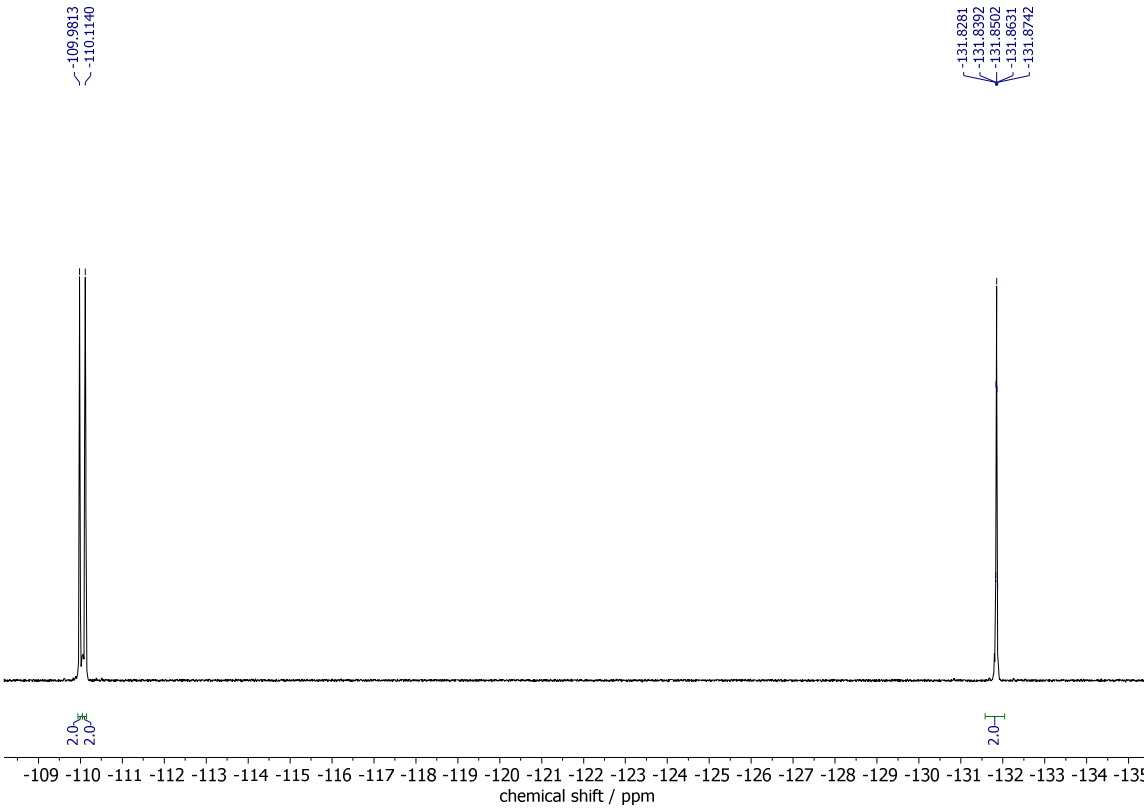

Figure S27. ^{19}F NMR spectrum (470 MHz) of **A3** in $CDCl_3$ at 298 K.

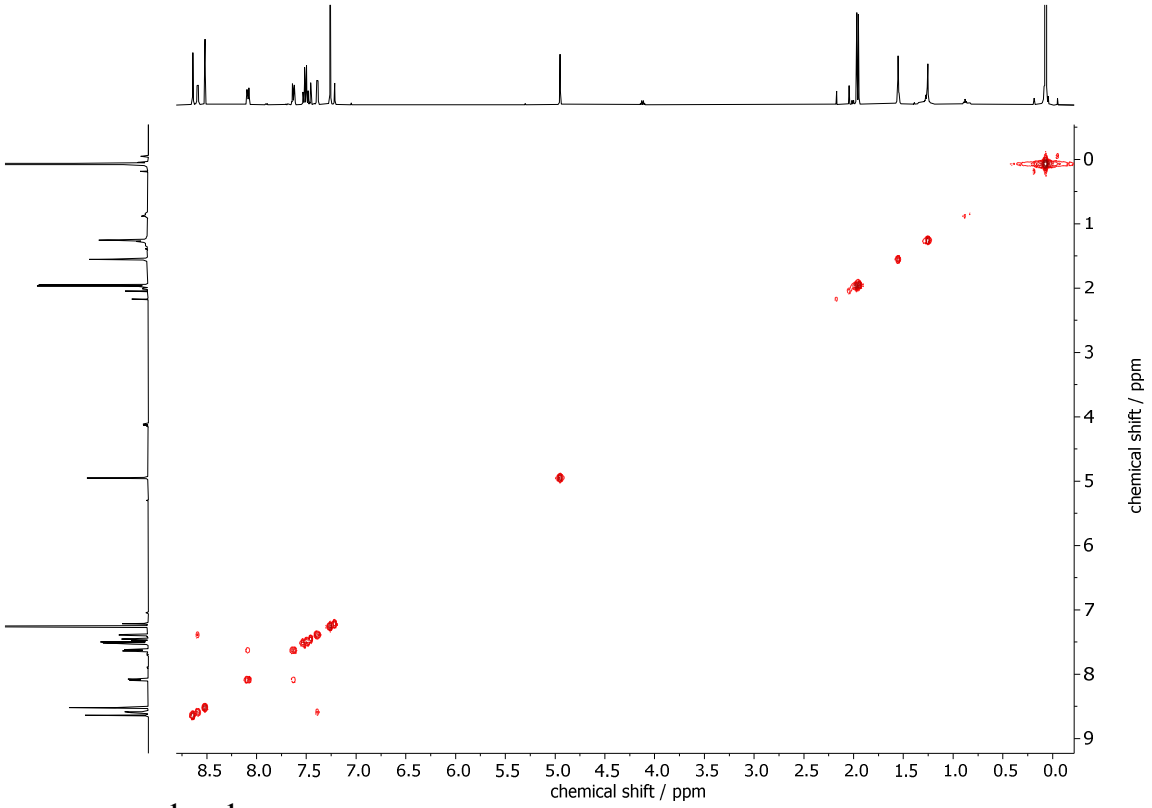

Figure S28. ^{1}H– ^{1}H COSY spectrum (500 MHz) of **A3** in $CDCl_3$ at 298 K.

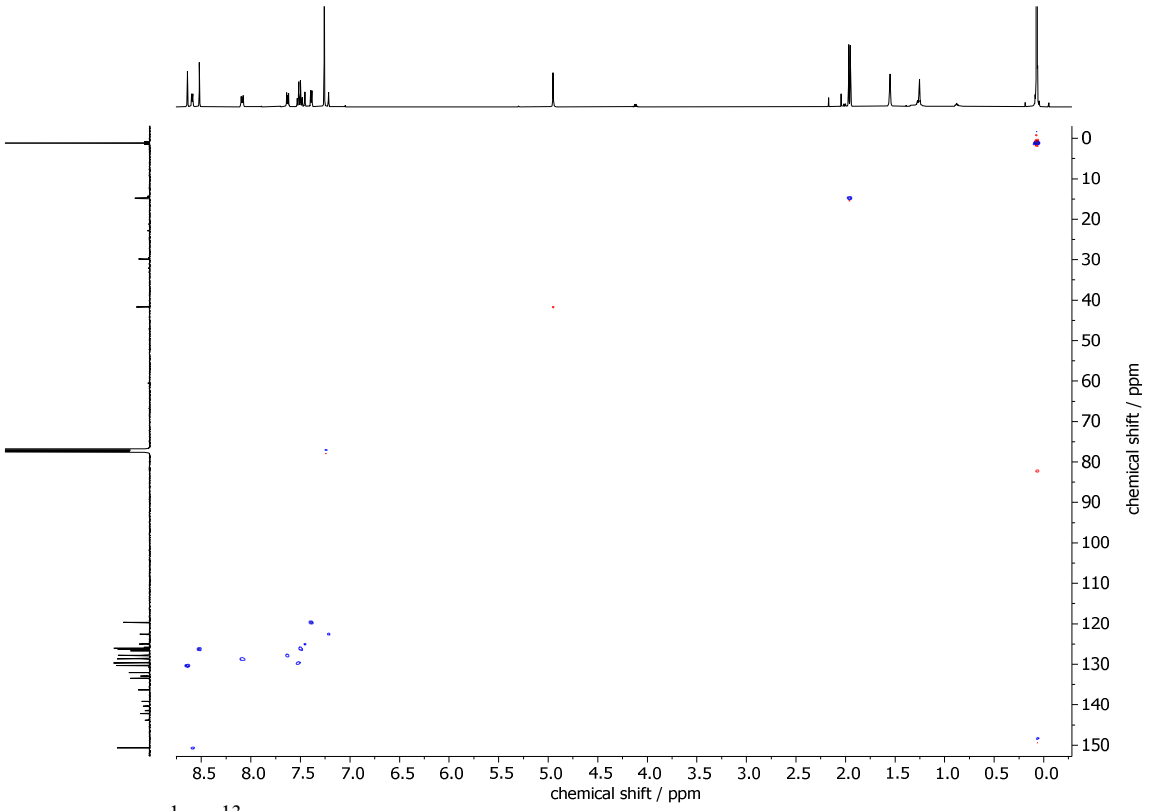

Figure S29. ^{1}H–^{13}C HSQC spectrum (500 MHz) of **A3** in $CDCl_3$ at 298 K.

4. Characterization by HRMS (ESI–QTOF)

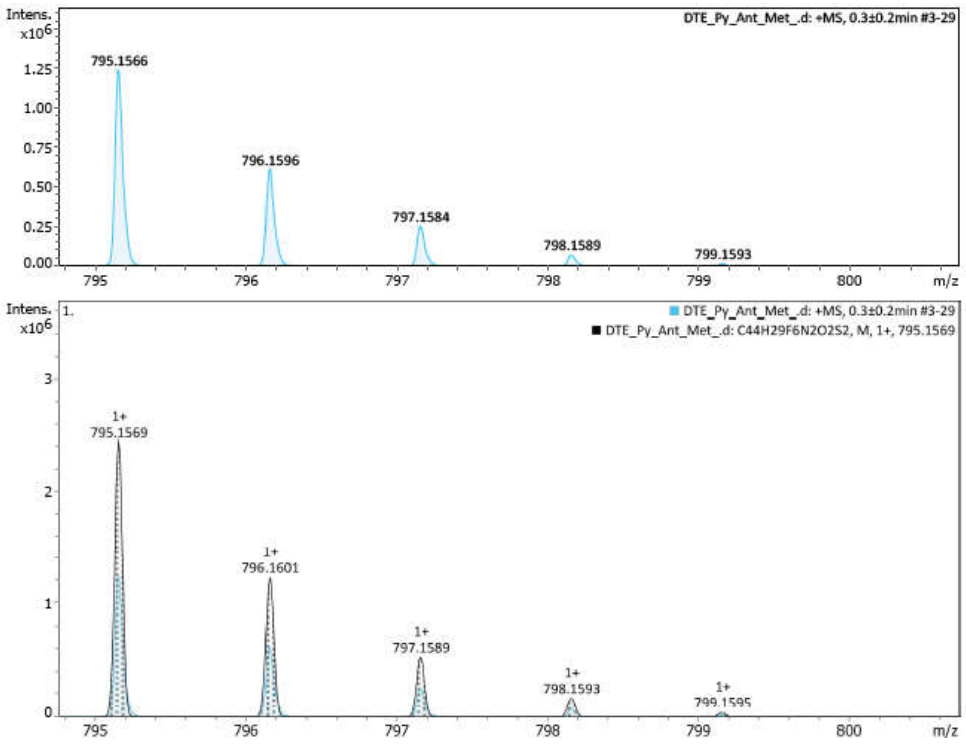

Figure S30. Top: HRMS (QTOF) spectrum of **1** in MeOH; positive mode. Bottom: Calculated isotopic pattern (overlapped in black).

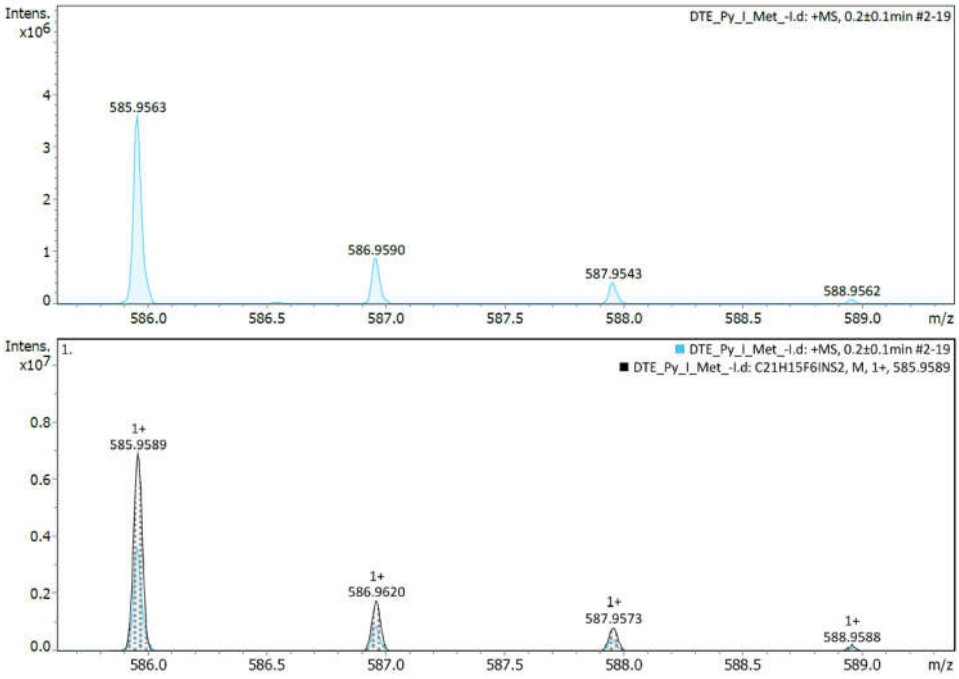

Figure S31. Top: HRMS (QTOF) spectrum of **2** in MeOH; positive mode. Bottom: Calculated isotopic pattern (overlapped in black).

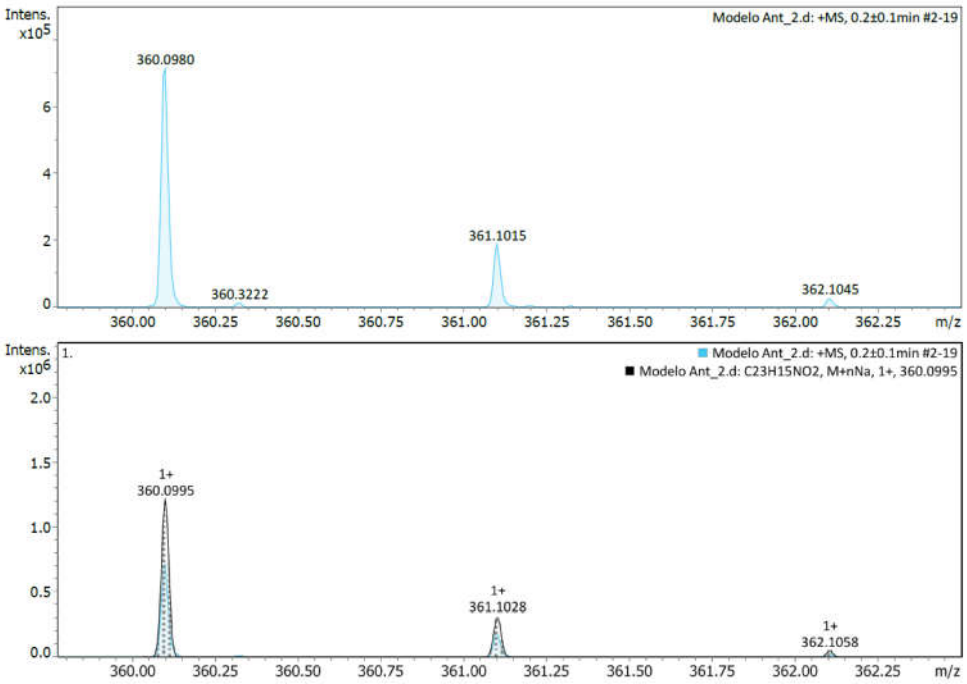

Figure S32. Top: HRMS (QTOF) spectrum of **3** in MeOH; positive mode. Bottom: Calculated isotopic pattern (overlapped in black).

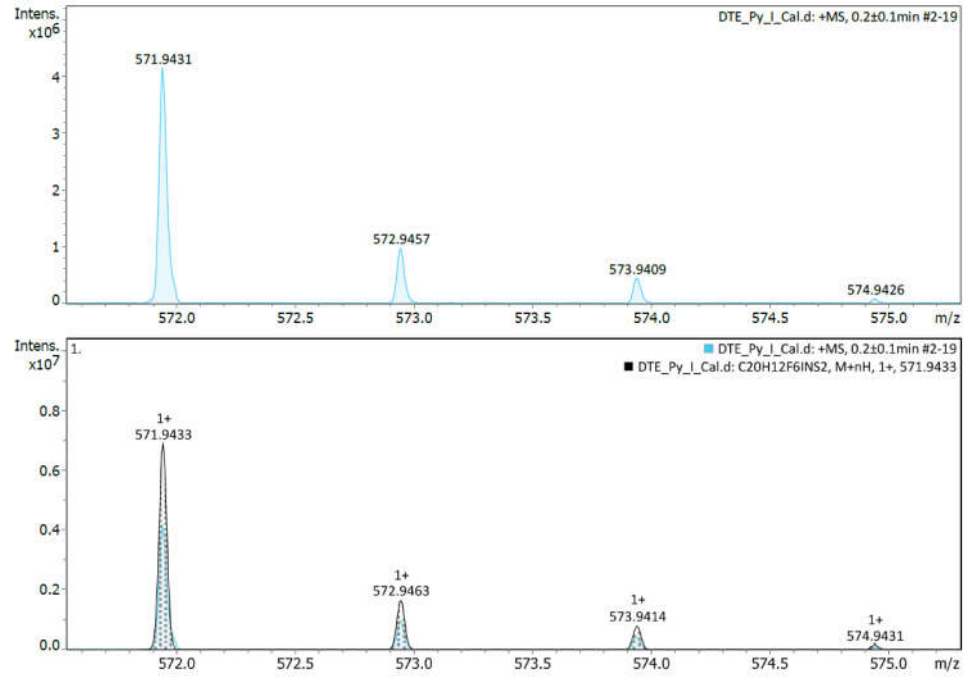

Figure S33. Top: HRMS (QTOF) spectrum of **A1** in MeOH; positive mode. Bottom: Calculated isotopic pattern (overlapped in black).

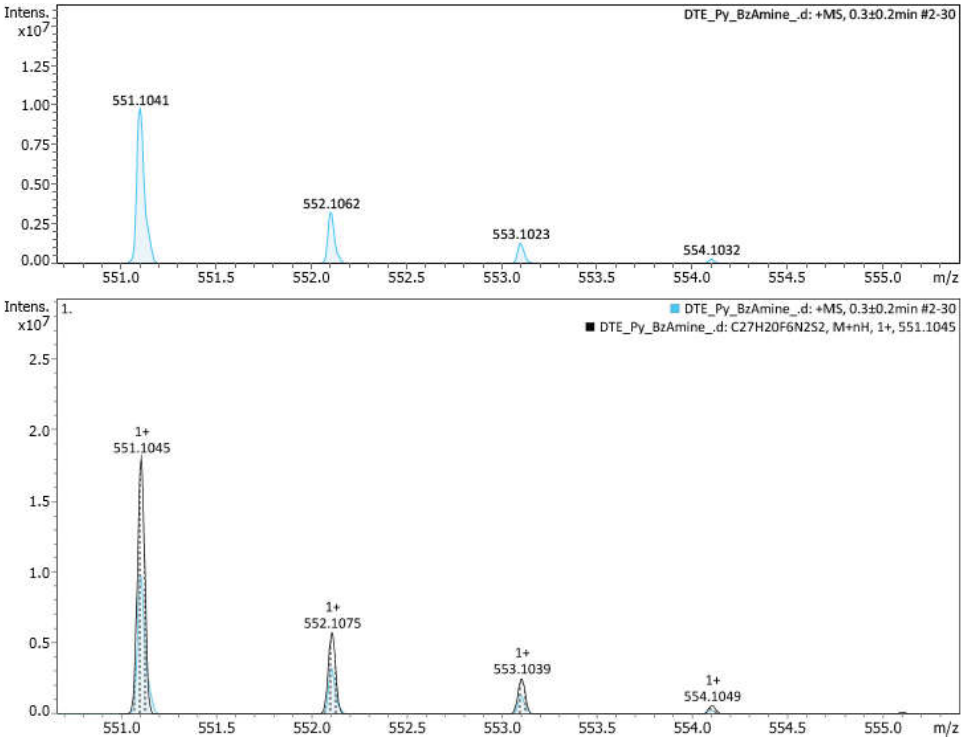

Figure S34. Top: HRMS (QTOF) spectrum of **A2** in MeOH; positive mode. Bottom: Calculated isotopic pattern (overlapped in black).

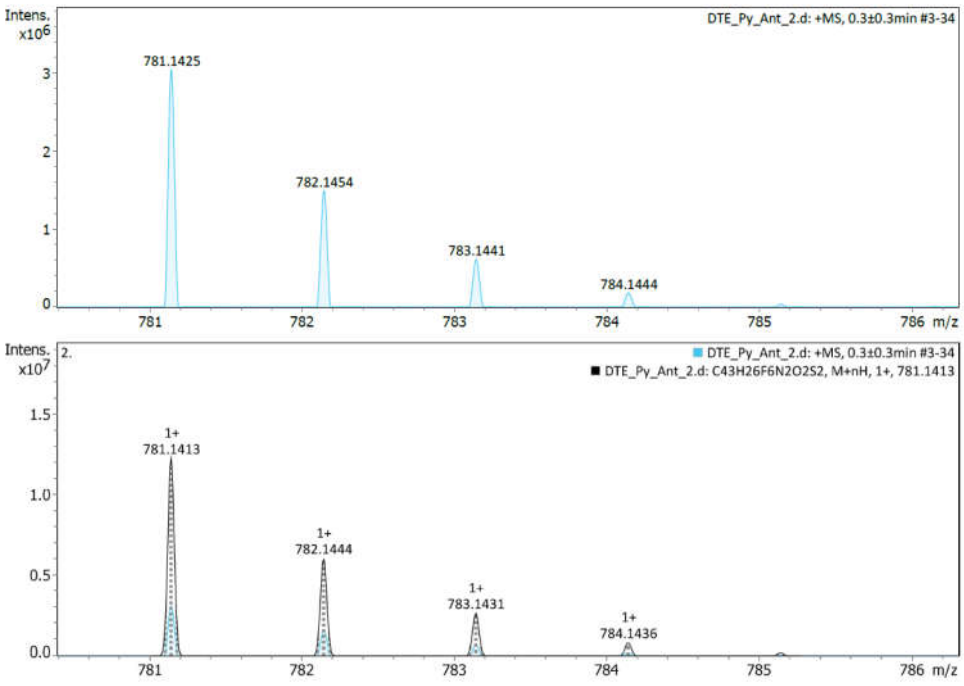

Figure S35. Top: HRMS (QTOF) spectrum of **A3** in MeOH; positive mode. Bottom: Calculated isotopic pattern (overlapped in black).

5. Photostationary state distribution (PSD)

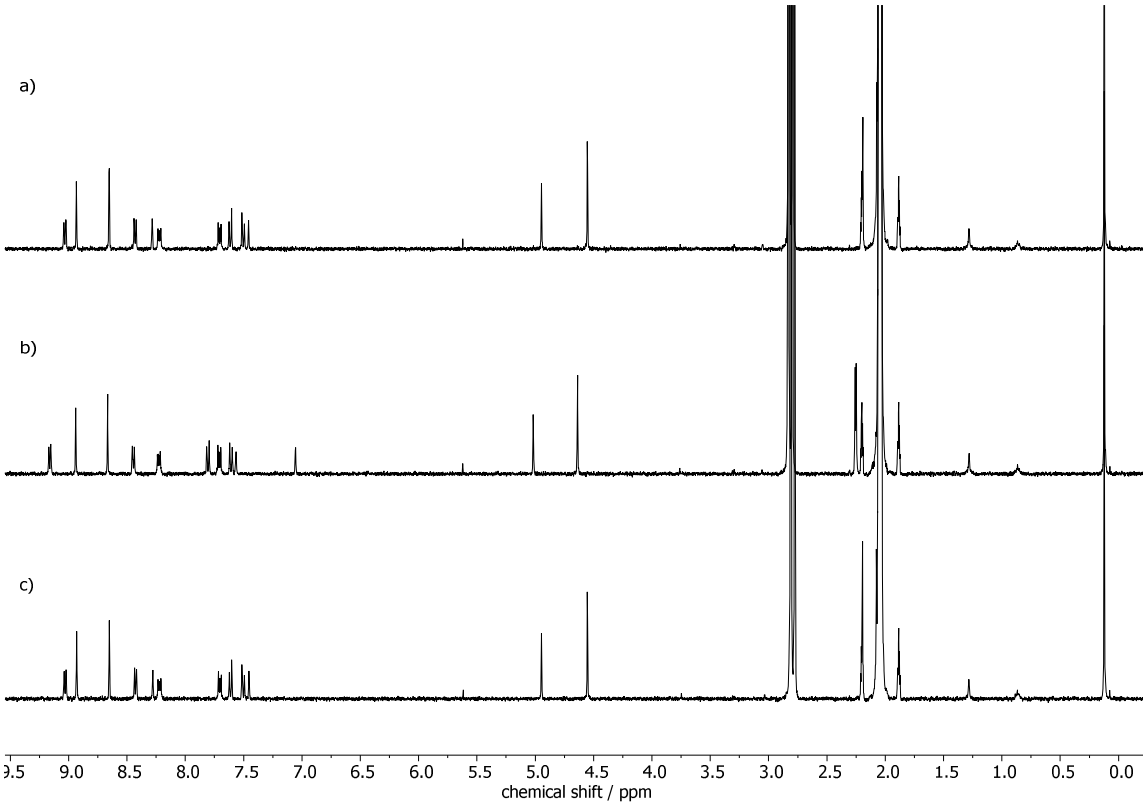

Figure S36. ^{1}H NMR spectra (400 MHz, 298 K, acetone-d_6) of (a) DTE **1o**, (b) DTE **1o** after irradiation for 30 min at 365 nm, and (c) DTE **1c** after irradiation for 60 min at > 550 nm (**1o**→**1c**:100%; **1c**→**1o**:100%).

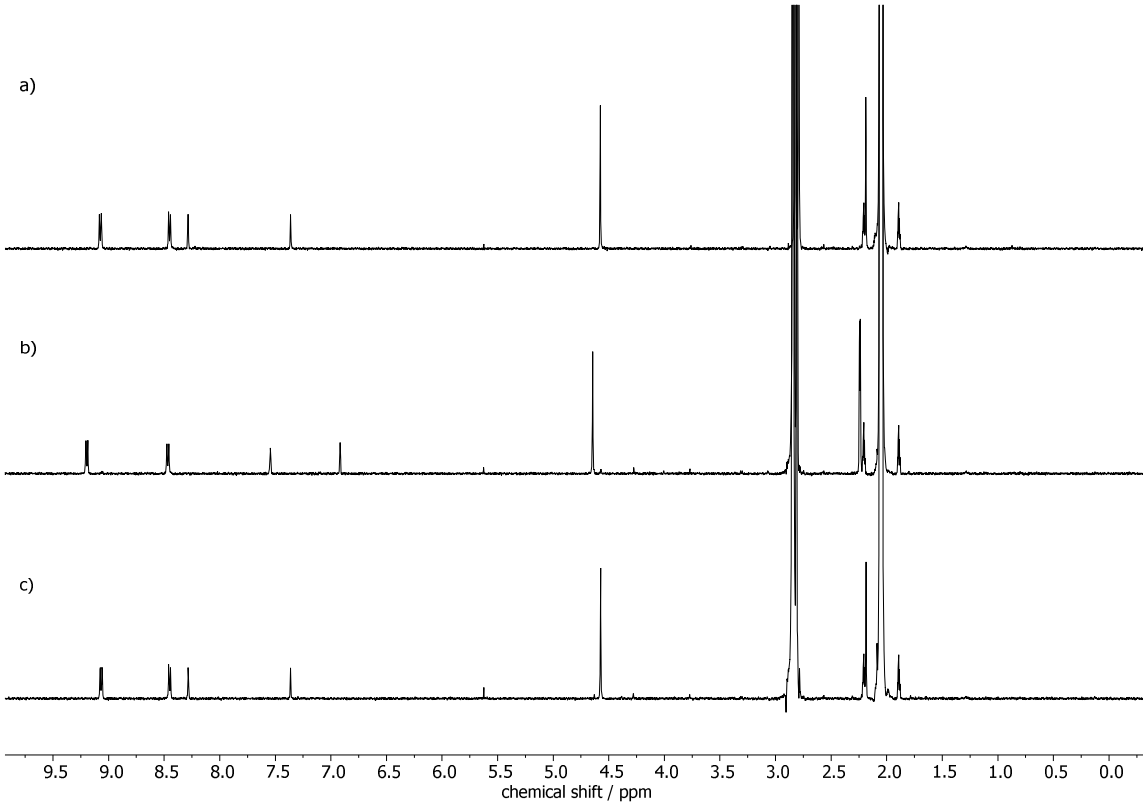

Figure S37. ^{1}H NMR spectra (400 MHz, 298 K, acetone-d_6) of (a) DTE **2o**, (b) DTE **2o** after irradiation for 20 min at 365 nm, and (c) DTE **2c** after irradiation for 30 min at > 495 nm (**2o**→**2c**:96%; **2c**→**2o**:100%).

6. Considerations about PeT pathways

The thermodynamic likelihood of photoinduced electron transfers in the dyads **1o** and **1c** was estimated with the Rehm-Weller equation:[8]

$\Delta G_{PeT} = E_{ox} - E_{red} - E^* + C$

being:

ΔG_{PeT} the free energy change associated to the concrete PeT process,

E_{ox} the oxidation potential of the electron donor (DTE_o or DTE_c),

E_{red} the reduction potential of the electron acceptor (*N*-methylanthracene-2,3-dicarboximide or *N*-methylpyridinium),

E^* the excitation energy of the selectively irradiated moiety (DTE_o, DTE_c or *N*-methylanthracene-2,3-dicarboximide),

C the Coulomb term (–0.06 eV).

The oxidation potential (*vs* SCE in acetonitrile) for the DTE (open and closed form) was approximated to the reported values for 1,2-bis(2-methyl-5-(4-methylphenyl)thien-3-yl)perfluorocyclopent-1-ene; E_{ox}(open) = +1.46 V and E_{ox}(closed) = +0.88 V.[9]

The reduction potential of *N*-methylanthracene-2,3-dicarboximide in acetonitrile was estimated relative to the reported value for the naphthalene analogue (E_{red} = −1.47 V *vs* Ag^+/Ag).[10] The upon extension of the π-system expected anodic shift of *ca*. 0.6–0.8 V is consistent with tabulated reduction potentials of polycyclic aromatic hydrocarbons.[11] This yields a conservatively predicted reduction potential of −0.9 to −0.7 V *vs* Ag^+/Ag (≈ −1.1 V *vs* SCE)[12] for *N*-methylanthracene-2,3-dicarboximide in acetonitrile. The reduction potential of the *N*-methylpyridinium cation is reported as E_{red} = –1.32 V (*vs* SCE in acetonitrile.[13] For practical reasons the offset of redox potentials between acetone and acetonitrile is assumed as being negligible.

The excitation energies of the DTE moiety were taken from the longest-wavelength maxima of the absorption spectra of **2o** and **1c** in acetone, corresponding 3.56 and 1.90 eV, respectively In the case of the anthracene moiety *E** was estimated from the absorption and fluorescence spectra of **3** in acetone (2.98 eV).

Applying the Rehm-Weller equation for each of the following PeT processes yielded the corresponding ΔG_{PeT} values.

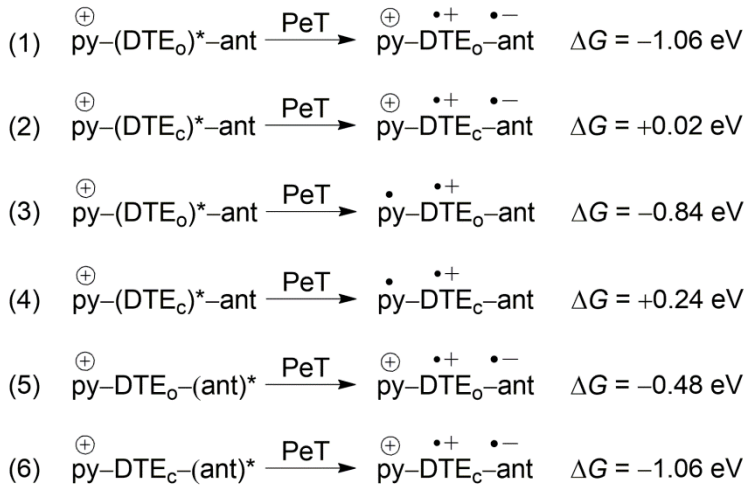

Please note that due to the obvious electron-accepting character of the pyridinium and the anthracene dicarboximide no oxidations of these moieties were considered.

7. References

1. R. W. Redmond and J. N. Gamlin, A compilation of singlet oxygen yields from biologically relevant molecules, *Photochem. Photobiol.*, 1999, **70**, 391-475.
2. C. Hatchard and C. A. Parker, A new sensitive chemical actinometer-II. Potassium ferrioxalate as a standard chemical actinometer, *Proc. R. Soc. London. Ser. A. Math. Phys. Sci.*, 1956, **235**, 518-536.
3. H. Kuhn, S. Braslavsky and R. Schmidt, Chemical actinometry, *Pure Appl. Chem.*, 1989, **61**, 187-210.
4. T. Sumi, Y. Takagi, A. Yagi, M. Morimoto and M. Irie, Photoirradiation wavelength dependence of cycloreversion quantum yields of diarylethenes, *Chem. Commun.*, 2014, **50**, 3928-3930.
5. M. Roseau, V. De Waele, X. Trivelli, F. X. Cantrelle, M. Penhoat and L. Chausset-Boissarie, Azobenzene: a visible-light chemical actinometer for the characterization of fluidic photosystems, *Helv. Chim. Acta*, 2021, **104**, 2100071.
6. S. Speiser, Photophysics and mechanisms of intramolecular electronic energy transfer in bichromophoric molecular systems: Solution and supersonic jet studies, *Chem. Rev.*, 1996, **96**, 1953-1976.
7. N. Sun, C. Wang, H. Wang, X. Gao and J. Jiang, Photonic switching porous organic polymers toward reversible control of heterogeneous photocatalysis, *ACS Appl. Mater. Interfaces.*, 2020, **12**, 56491-56498.
8. D. Rehm and A. Weller, Kinetik und Mechanismus der Elektronübertragung bei der Fluoreszenzlöschung in Acetonitril, *Ber. Bunsenges. Phys. Chem.*, 1969, **73**, 834-839.

9. M. Herder, B. M. Schmidt, L. Grubert, M. Pätzel, J. Schwarz and S. Hecht, Improving the fatigue resistance of diarylethene switches, *J. Am. Chem. Soc.*, 2015, **137**, 2738-2747.
10. Y. Kubo, T. Imaoka, T. Shiragami and T. Araki, A photoallylation of *N*-methylarenedicarboximides by allylsilanes, *Chem. Lett.*, 1986, 1749-1752.
11. M. Montalti, A. Credi, L. Prodi and M. T. Gandolfi, *Handbook of photochemistry*, CRC press, 2006.
12. V. V. Pavlishchuk and A. W. Addison, Conversion constants for redox potentials measured versus different reference electrodes in acetonitrile solutions at 25 ºC, *Inorg. Chim. Acta*, 2000, **298**, 97-102.
13. K. Y. Lee and J. K. Kochi, Charge-transfer structures of aromatic EDA complexes with *N*-heteroatom-substituted pyridinium cations, *J. Chem. Soc., Perkin Trans. 2*, 1992, 1011-1017.